

STUDIES ON OPTIMIZATION OF LAMINATED COMPOSITE PLATES

SHIV PRAKASH JOSHI



STUDIES ON OPTIMIZATION OF LAMINATED COMPOSITE PLATES

A Thesis Submitted
in Partial Fulfillment of the Requirements
for the Degree of
MASTER OF TECHNOLOGY

By
SHIV PRAKASH JOSHI

in the
DEPARTMENT OF AERONAUTICAL ENGINEERING
INDIAN INSTITUTE OF TECHNOLOGY, KANPUR

CERTIFICATE

This is to certify that the work STUDIES IN OPTIMIZATION
ON LAMINATED COMPOSITE PLATES has been carried out
under my supervision and has not been submitted elsewhere
for a degree.

W. G. B. 2-2-58
W. G. B. THORNTON
Professor
Department of Aero. Engrg.
I. I. T. Kanpur

POST GRADUATE CELL OFFICE The following has been received for the purpose of being examined for the degree of Master of Science in Engineering The student is the holder of the following degree from the following institution

CONTENTS

	Page
ABSTRACT	vi
LIST OF TABLES	vii
LIST OF FIGURES	viii
LIST OF SYMBOLS	x
CHAPTER 1 Introduction and Acknowledgments	1
1.1 Introduction	1
1.2 Literature Survey	1
1.3 Objective and Scope of the present work	2
CHAPTER 2 OPTIMAL DESIGN OF LAMINATED PLATES UNDER UNIFORM TENSILE COMPRESSION	3
2.1 Introduction	3
2.2 Optimization Procedure	10
2.3 Problem Formulation	11
2.3.1 Isogeoid	12
2.3.2 Derivative of Buckling Load	14
2.3.3 Constraints and their Gradients	16
2.4 Results and Discussion	17
2.4.1 Results	17
2.4.2 Discussion of Results	20
2.5 Conclusions	27

LIST OF TABLES

Table no.		Page
1.1	Effect of Number of Plys on maximum Buckling Load	15
1.2	Variation of Maximum Buckling Load with Aspect Ratio	15
1.3	Variation of Maximum Buckling Load with Eccentric Loading Ratio	21
1.4	Optimum Buckling Load considering Thickness and Fiber Orientation as Design Variables	23
1.5	The Optimum Values of the Ply Thickness and Corresponding Fiber Orientation for a Plate (with only transverse loading applied)	25
1.6	Variation of Optimum Values with Aspect Ratio and Uniaxial Loading Ratio	29
4.1	Variation in the Optimum Weight with change in pre-assigned alternates Fiber Orientation	41
4.2	Variation in the Optimum Ply Thickness with Total Number of Plyies	53

Table no.		Page
4.3	Variation in the Optimum Ply Thickness with Total Number of Plies	84
4.4	Variation in Ply Thickness with change in pre-designed Fiber Orientation	85
4.5	Variation of Optimum Fiber Orientation and corresponding Thickness	86
4.6	Optimum Fiber Orientation and Corresponding Ply Thickness	87

LIST OF FIGURES

Figure No.		Page
1.1 (a)	Co-ordinate system & fiber orientation	25 (a)
1.1 (b)	Stacking sequence & co-ordinate system for the layered plate.	25 (b)
1.2	Variation of Buckling Load with Fiber Orientation	26
1.3	Variation of Buckling Load with Fiber Orientation	27
1.4	Change in Fiber Orientation during Optimization	28
1.1	Maximum Deflection of simply supported Laminated Plate vs. Fiber Orientation	35
1.2	Variation of Longitudinal Stress with Fiber Orientation	36
1.3	Variation of Transverse Stress with Fiber Orientation	37
1.4	Variation of Shear Stress with Fiber Orientation	38
1.5	Variation of Optimum Weight with Aspect Ratio	39
1.6	Variation of Deflection and Buckling Load with Aspect Ratio for Optimum Weight Design	70

Figure No.		Page
3.5	Variation of Optimum Weight with Diurnal Loading Ratio	31
4.1	Optimum Ratio vs. Total Number of Piles	38

LIST OF SYMBOLS

a, b	: Dimensions of the plate
A_{ij}, B_{ij}, D_{ij}	: Elastic constants of the composite plate
X_x, X_y	: In-plane normal forces
X_x^u	: Lower limit on Machlin's load per unit width
X	: Ratio of in-plane normal forces (X_y/X_x)
\bar{E}_{ij}	: Reduced stiffnesses evaluated at fiber orientation angle.
q	: Lateral loading
t_i	: Thickness of i^{th} lamina
u, v	: In-plane displacements
w	: Lateral displacement
$\epsilon_x, \epsilon_y, \epsilon_{xy}$: Strain components in the xy-plane
$\sigma_x, \sigma_y, \sigma_{xy}$: In-plane stresses
θ	: Fiber orientation of i^{th} lamina
n_i	: Design variables
N	: Total number of design variables
L	: The number of plies in laminae

STUDIES ON OPTIMIZATION OF LAMINATED COMPOSITE PLATES

DRIV PROGRAM 1981

M. Tech. Thesis

Department of Aeronautical Engineering

Indian Institute of Technology, Delhi

ABSTRACT

Studies are carried out for the minimum weight optimum design of laminated fiber composite plates, subjected to multiple inplane loadings and transverse loadings. The behaviour constraints are on stability, strength and deflection. Angle-ply laminates with orthotropic laminae and orthotropic angle-ply laminates are considered for optimization studies. The orthotropic property is achieved by taking an equal number of fibers at positive and negative orientations, with respect to structural axis in the former case. Thickness of plate and corresponding fiber orientations are discretized as design variables while the number of plies is treated as a design parameter. The constrained optimization problem is transformed into a series of unconstrained optimization problems, using an interior penalty function approach. The results have been obtained for different aspect ratios and uniform biaxial inplane loading ratios. This study shows that the fiber orientations

of thicknesses near optimum have little effect on the optimum design. There exists a particular fiber orientation angle for the overall thickness of laminate, which results in the optimum design for a plate of a given aspect ratio under a given set of loadings. In case of antisymmetric angle-ply laminates, particular ratios of ply thickness result in the optimum design of the plate. It has been observed that the number of plies have no effect on the optimum design.

REVIEW

INTRODUCTION AND SCOPE OF REVIEW

1.1 INTRODUCTION

During the last two decades or so, fiber reinforced laminates have found increasing applications in many engineering structures. They are largely used in aeronautical industries for both primary and secondary structures. The fiber reinforced composites possess two desirable features: one is their high stiffness-to-weight and strength-to-weight ratio, and the other is their anisotropic mechanical property that can be tailored through variation of the fiber orientation, thickness of plies and stacking sequence - a feature which gives the designer an added degree of flexibility to achieve the desired strength or stiffness in any direction. The ever-increasing use of composites have stimulated interest in the development of optimal design of structures made of composite materials.

Laminated plates constitute an important structural element in aerospace, mechanical and electrical industries. Laminated fibrous composites are a class of composites involving both fibrous composites and lamination techniques. Here, layers of fiber reinforced material are built up with the fiber direction of each layer typically oriented in different direction to give different strengths and stiffnesses in the various directions, as desired by the

designer. Examples of laminated fiber reinforced composites include aerospace vehicles/ space covering, missile cases, aircraft wing panels and body sections, rocket nozzles, heat shields, fiber-glass boat hulls, tennis rackets, golf club shafts-etc..

In aerospace applications, where weight saving is of paramount importance, the advent of high modulus/ high-strength fiber reinforced composite materials such as carbon/epoxy and graphite/epoxy, has resulted in a dramatic increase in the use of laminated fiber reinforced plates and other structural shapes as primary structural members. The past, present and future of the composite is already and being studied and the evolution is as follows: the advanced composites were developed around 1960 and then the conceptual and structural investigations were demonstrated. Up to 1975, small components of hardware had been developed and flight tested. At present, large primary structures are being investigated. The latest journals reveal that there plans to build airplanes by using up to 50 percent composite materials. The final stage is the all-composite airplanes which will be seen in the near future. To achieve this, recently, optimization techniques have been applied to get optimal weight design with desirable structural properties.

In the next section, a survey of the existing literature pertaining to optimization is presented.

1.2. REINFORCED CONCRETE

Optimization in concrete structural design was recognized as early as 1970, references⁽¹²⁻¹³⁾ dealt with optimal use of reinforced concrete, sufficient to strength as a design criterion.

Arat et. al.⁽¹⁴⁾ suggested an efficient optimization method based on strain energy minimization and a conjugate search for the minimum weight design of reinforced concrete shear reinforced composite. The optimum design procedure takes into consideration multiple loading conditions and displacement constraints in the structure, various sections consisting of both isotropic and composite elements are solved and the results tabulated.

Lai and Schleich⁽¹⁵⁾ used a direct search procedure to optimize layered structures, subjected to dynamic loading conditions. The technique is applied to problems of optimal design for minimum tensile stress in the segments in layered structures, under time harmonic loads and transient loads respectively.

Schmit and Kirsch⁽¹⁶⁾ presented a method for minimum weight design of symmetric composite structures subjected to multiple in-plane loading conditions, which take into account composite stiffness requirements and

orthotropic laminations. The problem is cast as a nonlinear mathematical programming problem in which the thickness of material is a design variable with unassigned orientation angles.

Valasek et al. [1] applied optimality criteria in the iterative reanalysis of the elements of finite element model to achieve minimum weight. The program normally accepts a single generalized deflection constraint, but multiple constraints can be accommodated in any cases of practical interest by multiple reanalyses/program.

Choi [2] wrote a computer program (COLLAPSE) which can be used to optimize or analyze a composite structure. Response of the structure to the applied loads is obtained by finite element analysis. The design variables are modified during each iteration by using a recurrence relation. The four strength criteria included in the program are:

maximum stress, maximum strain, Hill's criterion modified by Von-Mises and Morris criterion. The plate elements can be designed to prevent local buckling.

Wang [3] presented an algorithm based on the simplex method of linear programming, without linearizing the non-linear mixed integer programming problem involving the number of layers, their thicknesses and their fiber directions. Orthotropic layers were used and the deformations of the

analysis showing that the layers lie symmetric about the mid plane of the laminate. It is assumed that fibers are available in such a range of thickness such that weight always be constant.

Holmes (1981) dealt with the problem of optimizing multi-layer fiber reinforced sections. The formulation variables are the total deflection of the finite element model. It is shown that program is convenient for solving the nonlinear mixed integer problem involved and allows the optimal number of layers in each direction. The layer thickness and the fiber angle were determined simultaneously for very general inequality constraints on stress and deflections.

Chen et. al. (1982) determined optimum orientation for a symmetric composite laminate consisting of layers of $+45^\circ$ and -45° fiber orientations and subjected to in-plane loadings. Stability of both the laminate and laminate ply are evaluated. The buckling results presented are restricted to specially orthotropic laminates while the first laminate ply is assumed to initiate laminate failure.

Schmit and Jurehi (1983) presented a method for the minimum weight optimum design of laminated fiber composite plates, subjected to multiple in-plane loading conditions.

which include stiffness, strength, and elastic stability constraints. The buckling analysis is based on an equivalent orthotropic plate approach. This approach is appropriate for heavily loaded, balanced, symmetric laminates involving relatively large number of plies. The optimization technique used is a sequence of linear programming techniques with constraint deletion technique in conjunction with Taylor series approximations for the constraints. Thickness of plies and number of plies are used as design variables while fiber orientation is prescribed.

Hayashi (14) presented optimum design of plyered beds of angle ply laminates. The fiber orientations are optimized for the corresponding buckling strength. However, he neglected the thickness of the laminate to be preassigned.

Hinson (15) carried out the optimum design of laminated plates with orthotropic layers under uniaxial and biaxial compression. Anisotropy is achieved by using equal number of fibers with $+\theta$ and $-\theta$ orientation in the same ply. Laminated plate is made up of plies with equal thickness. Layer thickness of each ply is assigned as design variable while the number of plies is preassigned. Possible conjugate direction method is used to maximize the buckling stress.

Recently Shogren et. al. [24] have shown that, with variable thickness of plys, the degrading effect of coupling can be diminished. This results in an increase in the strength of the laminate.

The survey of the foregoing literature on the optimum design of laminated composite plates shows that, not all the design variables have been included to arrive at an optimal design. Fiber fiber orientation or thickness of a ply has been included as a design variable. Thus it seems a systematic study of optimization of composite plates is required by taking into account all the possible design variables.

1.3 CONTINUOUS AND DISCRETE OR FIBER ORIENTATION, LAM

The design problem with composites involves the determination of thickness distributions and corresponding fiber orientations. Thickness for each fiber orientation can always be subdivided into integer number of plys with given fiber orientation (this may be necessary because of manufacturing limitations). The penalty paid by slight variation in thickness in order to get integer number for plys can be exploited, which may not occur when the plates with preassigned thickness or constraints on the number of plys to be an integer. The thickness distribution and corresponding fiber orientation should be chosen:

in such a way, that an optimal solution is obtained for a desired objective, like minimum weight, at the same time behavioral constraints like plate stability, etc., and also constraints which involve manufacturing techniques and available gauge sizes, etc., be satisfied. If the objective function or the design requirements are dependent on other design variables or on a complex analysis, the optimization problem becomes very difficult. This, unfortunately, is the optimum design of laminated composites (Gupta).

In the present work, an attempt is made to incorporate thickness of each ply and fiber orientation as design variables, while the number of plies is used as a design parameter. The types of problems are studied:

- (I) Optimum design of a layered composite plate of a given dimension to have a maximum buckling load,
- (II) Minimum weight design of the laminate subjected to in-plane and transverse loading.

In both the problems analytical derivatives are obtained. Interior penalty function approach is used for sequential unconstrained optimization using Goldfarb's modification of the Fletcher - Powell method for unconstrained optimization with Goldfarb's method for additional steps.

A study of the buckling under biaxial compression is presented in Chapter 2. Buckling load is obtained to understand the behavior of fiber orientations. The second problem in chapter 2 incorporates thickness of each ply in addition to the fiber orientation as design variables.

Chapter 3 deals with an optimum weight design of composite plate under in-plane and transverse loadings. Composite plate created with orthotropic laminae is considered. Each lamina's principal directions coincide with structural axes.

Antisymmetric angle-ply laminates are considered in chapter 4. For optimization studies with constraints on stress, deflection and buckling load.

Chapter 5 summarizes the results of the investigation. A short note is added to indicate the extension of the present work.

CONCLUSIONS

~~Research in the field of anisotropic~~

~~materials has been carried out~~

2.1. Introduction:

Since the early 1950's the use of anisotropic fiber reinforced composites as structural materials has increased considerably (1). This increase owes to the fact that the designer can take advantage of the anisotropic properties of the materials. The knowledge of anisotropic composite materials in the form of thin plates, subjected to in-plane compressive loads, are of particular interest. The primary role of many of these plates is bending under axial compression. By applying optimization techniques, one can get an optimum design and thereby use these materials quite efficiently.

The present study is an attempt to understand the behavior of the plate with varying thickness of the lamina and corresponding fiber orientation. A composite laminated plate, with uniaxially oriented having anisotropic property, is employed. Anisotropy is achieved by using equal number of plies at $+45^\circ$ and -45° with respect to structural axis. Bending and shear are uncoupled for each ply. The reduced stiffness coefficients, \bar{E}_{11} and \bar{E}_{22} , are identically zero. In this case, principal material directions and structural directions coincide.

The study is carried out for the following:

- (1) Optimization of a layered composite plate for maximum buckling load with constraint on each ply to be within a prescribed thickness.
- (2) Optimization of a layered composite plate for maximal buckling load with constraint on the total thickness of laminae to be within a prescribed value.

2.2. Formulation of the problem

The constrained optimization problem considered herein is to find a vector of design variables, \mathbf{w} , that minimizes the buckling load, $P_{cr}(\mathbf{w})$, as a function, subject to the constraints

$$G_i(\mathbf{w}) \geq 0 \quad i = 1, 2 \quad (1)$$

It is assumed that at least one of the constraints of Eq. (1) is active at the optimal point, that is, $G_i(\mathbf{w}) = 0$ for some i . This constrained optimization problem may be transformed into a series of unconstrained minimization problems by introducing a penalty function associated with the constraints. In the transformed problem, we have to find the maximum of a function $P(\mathbf{w})$ as r approaches zero, where

$$P(\mathbf{w}, \mathbf{w}) = P_{cr}(\mathbf{w}) + r \sum_{i=1}^2 \delta_i(\mathbf{w}) \quad (2)$$

$z_1(v)$ is defined here as

$$z_1(v) = \ln [q_1(v) / (1 - q_1(v))] \geq 0 \quad (31)$$

The term $z_1(v)$ represents the penalty associated with the 1^{st} constraint in an interior penalty function. In the sense that it is defined only if v lies in feasible design domain, the above constrained problem can be solved by a sequence of unconstrained minimization problem, by Fletcher and Powell method [18].

2.2.2. Objective Function

For the present investigation the objective function is

$$\text{Max } f_{10}(\omega_{10}, t_1) \quad i = 1, 8$$

such that

$$0 \leq \omega_{10} \leq \omega_{10}^{\max} \quad t_1 \geq 0$$

$$\text{and} \quad (i) \quad t_1 \leq t_1^{\max} \quad i = 1, 8 \quad (32)$$

$$(ii) \quad \sum_{i=1}^8 t_i \leq t^{\max}$$

These constraints are suitably formulated to fit in the interior penalty function approach.

2.3.1. Nonlinear

Fig. 1.1 (a) shows an orthotropic ply with equal number of +45 and -45 fiber orientations. It should be noted that \bar{U}_{12} and \bar{U}_{22} are identically zero.

The three governing equations along x,y and z are (18)

$$\begin{aligned} \sigma_{11} \epsilon_{xx} + \sigma_{22} \epsilon_{yy} + \phi_{11} + \lambda_{22}^2 \epsilon_{xy} - 2\lambda_{11} \epsilon_{xx} \\ - \phi_{11} + 2\lambda_{22}^2 \epsilon_{xy} = 0 \end{aligned} \quad (15)$$

$$\begin{aligned} \phi_{12} + \lambda_{22}^2 \epsilon_{xy} + \sigma_{22} \epsilon_{xx} + \lambda_{22} \epsilon_{yy} = (\lambda_{12} + 2\lambda_{22}^2) \\ \epsilon_{xy} - \lambda_{11} \epsilon_{yy} = 0 \end{aligned} \quad (16)$$

$$\begin{aligned} \lambda_{11} \epsilon_{xxx} + 2 (\lambda_{12} + 2\lambda_{22}^2) \epsilon_{xyy} + \lambda_{22} \epsilon_{yyy} \\ - \lambda_{11} \epsilon_{xxx} - (\lambda_{12} + 2\lambda_{22}^2) \epsilon_{xyy} - \lambda_{12} + 2\lambda_{22}^2 \epsilon_{xy} \\ - \lambda_{22} \epsilon_{yyy} + \lambda_{22} \epsilon_{xx} + \lambda_{22} \epsilon_{yy} = 0 \end{aligned} \quad (17)$$

where (see fig. 1.1(b))

$$\begin{aligned} \sigma_{11} &= \sum_{k=1}^2 (\bar{U}_{11})_k (\epsilon_k - \epsilon_{k-1}) \\ \sigma_{22} &= \frac{1}{2} \sum_{k=1}^2 (\bar{U}_{22})_k (\epsilon_k^2 - \epsilon_{k-1}^2) \\ \sigma_{12} &= 1/2 \sum_{k=1}^2 (\bar{U}_{12})_k (\epsilon_k^2 - \epsilon_{k-1}^2) \end{aligned} \quad (18)$$

and

$$\lambda_{ij} = \lambda_{ji}$$

Still now the problem is quite general and can be applied to any boundary conditions. For example the analysis is restricted to simply supported boundary conditions, which are used for optimization studies. To choose u, v , and w in the following manner to satisfy simply supported boundary conditions,

$$\begin{aligned} u &= \bar{u} \cos (n \pi x/a) \sin (m \pi y/b) \\ v &= \bar{v} \sin (n \pi x/a) \cos (m \pi y/b) \\ w &= \bar{w} \sin (n \pi x/a) \sin (m \pi y/b) \end{aligned} \quad (9)$$

Substituting these selected functions (9) in the governing equations (3,4,7), and further simplification arrives at

$$\begin{aligned} X_{ij} = & \frac{1}{a^2 b^2} \left[\frac{1}{n^2 + m^2} \frac{1}{(a_n/b_m)^2} \left(\tau_{11} + \right. \right. \\ & \left. \left. \frac{2 \tau_{12} \tau_{23} \tau_{13} - \tau_{23}^2 \tau_{13}^2 - \tau_{11} \tau_{22}^2}{\tau_{11} \tau_{22} - \tau_{12}^2} \right) \right] \quad (10) \end{aligned}$$

where

$$\begin{aligned} \tau_{11} &= A_{11} a^2 \pi^2 + A_{55} a^2 x^2 (a/b)^2 \\ \tau_{12} &= A_{12} + A_{55} x a \pi^2 (a/b) \\ \tau_{13} &= A_{11} a^2 \pi^2 + (A_{12} + 2 A_{55}) a x^2 (a/b)^2 \\ \tau_{22} &= A_{22} a^2 \pi^2 + A_{55} a^2 \pi^2 (a/b)^2 \end{aligned}$$

$$\begin{aligned} \sigma_{22} &= B_{12} + 2k_{22}^2 \pi^2 (a/b) + B_{22} \pi^2 (a/b)^2 \\ \sigma_{33} &= B_{12} \pi^4 \pi^4 + 2 (B_{12} + 2k_{22}^2) \pi^2 a^2 \pi^4 (a/b)^2 \\ &\quad + B_{22} \pi^4 \pi^4 (a/b)^2 \end{aligned}$$

2.1.2. ANALYSIS OF LAMINATE LAY

The application of optimization algorithm requires the problem of objective function and constraints. Numerical computation leads to two function evaluation at each design point which leads to higher computational time. Because of the complex nature of the function, truncation errors increase and hence produce erroneous which gradients/decreases the efficiency of the algorithm. Derivatives of critical mass load with respect to design variables, which include thickness of ply and corresponding orientations, are obtained as follows.

Let v_i be design variable $i = 1, 2$

For this case,

$$v_1 = t_1 \quad i = 1, \quad h'/2 \quad \text{and} \quad v_2 = \theta_1 \quad 180'/2+1.8'$$

Differentiation of σ_2 , (15) gives,

$$\begin{aligned} \frac{\partial \sigma_2}{\partial v_1} &= \frac{1}{\pi^2 a^2 \{ a^2 + 2k_{22}^2 (a/b)^2 \}} \left[\frac{\partial \sigma_{22}}{\partial v_1} \right. \\ &\quad \left. + (v_{11} v_{22} + v_{12}^2) \frac{\partial \sigma_{12}}{\partial v_1} + v_{22} v_{33} + 2 \frac{\partial \sigma_{23}}{\partial v_1} v_{12} v_{33} \right] \end{aligned}$$

Scanned with
 CamScanner
 www.camscanner.com

$$\begin{aligned}
& + 2 \frac{\partial^2 \pi_{12}}{\partial v_1^2} v_{22} v_{12} = \frac{\partial^2 \pi_{22}}{\partial v_1^2} v_{12}^2 + 2 \frac{\partial^2 \pi_{12}}{\partial v_1^2} v_{12} \\
& - \frac{\partial^2 \pi_{12}}{\partial v_1^2} v_{22}^2 + 2 \frac{\partial^2 \pi_{22}}{\partial v_1^2} v_{11} v_{22} = (2 v_{12} v_{22} \frac{\partial^2 \pi_{12}}{\partial v_1^2} \\
& - v_{22} v_{12}^2 - v_{11} v_{22}^2) + (\frac{\partial^2 \pi_{12}}{\partial v_1^2} v_{22} + \frac{\partial^2 \pi_{22}}{\partial v_1^2} v_{11} \\
& - 2 \frac{\partial^2 \pi_{12}}{\partial v_1^2} v_{12})^2 + (v_{22} v_{22} - v_{12}^2)^2 \quad (12)
\end{aligned}$$

where,

$$\begin{aligned}
\frac{\partial^2 \pi_{12}}{\partial v_1^2} &= \frac{\partial^2 \pi_{12}}{\partial v_1^2} m^2 v^2 + \frac{\partial^2 \pi_{22}}{\partial v_1^2} m^2 v^2 (a_0/b)^2 \\
\frac{\partial^2 \pi_{12}}{\partial v_1^2} &= (\frac{\partial^2 \pi_{12}}{\partial v_1^2} + \frac{\partial^2 \pi_{22}}{\partial v_1^2}) m m v^2 (a_0/b) \\
\frac{\partial^2 \pi_{12}}{\partial v_1^2} &= \frac{\partial^2 \pi_{12}}{\partial v_1^2} m^2 v^2 + (\frac{\partial^2 \pi_{12}}{\partial v_1^2} + 2 \frac{\partial^2 \pi_{22}}{\partial v_1^2}) m m v^2 (a_0/b)^2 \\
\frac{\partial^2 \pi_{22}}{\partial v_1^2} &= \frac{\partial^2 \pi_{22}}{\partial v_1^2} m^2 v^2 + \frac{\partial^2 \pi_{22}}{\partial v_1^2} m^2 v^2 (a_0/b)^2 \quad (13) \\
\frac{\partial^2 \pi_{22}}{\partial v_1^2} &= (\frac{\partial^2 \pi_{12}}{\partial v_1^2} + 2 \frac{\partial^2 \pi_{22}}{\partial v_1^2}) m^2 v^2 (a_0/b) \\
&+ \frac{\partial^2 \pi_{22}}{\partial v_1^2} m^2 v^2 (a_0/b)^2 \\
\frac{\partial^2 \pi_{22}}{\partial v_1^2} &= \frac{\partial^2 \pi_{12}}{\partial v_1^2} m^2 v^2 + 2 (\frac{\partial^2 \pi_{12}}{\partial v_1^2} + 2 \frac{\partial^2 \pi_{22}}{\partial v_1^2}) m^2 v^2 v^2 \\
&(a_0/b)^2 + \frac{\partial^2 \pi_{22}}{\partial v_1^2} m^2 v^2 (a_0/b)^4
\end{aligned}$$

Gradients of k_{1j} , k_{2j} and u_{1j} of Eq. (13) have been referred at various stages in this thesis. These stiffness matrices are a function of, both fiber orientation and thickness of ply. Expressions for gradients of stiffness matrices are given in Appendix 1.

1.1.1. FIRST OPTIMIZATION PROBLEM

Constraints and their derivatives for the optimization studies carried out are as follows :

Following constraints are imposed on the first problem

$$G_1 = 1 - \gamma_1 / \gamma_1^0 \quad i = 1, 2, 3 \quad (14)$$

$$G_2 = 1 - \gamma_2 / \gamma_2^0 \quad i = 2, 3, 4 + 1, 2, 3 \quad (15)$$

and

$$u_1 - u_1^0 = 0 \quad i = 1, 2 \quad (16)$$

Derivatives of equations 14,15 and 16 are as follows

$$\frac{\partial G_1}{\partial \gamma_j^0} = -\delta_{1j} \quad 1/\gamma_1^0 \quad \text{for } i = 1, 2, 3 \quad j=1, 2 \quad (17)$$

$$\frac{\partial G_2}{\partial \gamma_j^0} = -\delta_{2j} \quad 1/\gamma_2^0 \quad \text{for } i=3, 4+1, 2, 3 \quad j=1, 2 \quad (18)$$

Following constraints are imposed on the second problem.

$$G_1 = 1 - \left(\sum_{j=1}^{M/2} \gamma_j \right) / \gamma_1^0 \quad (19)$$

$$G_1 = 1 - \frac{V_f + 1}{11/2} \frac{E^* E_1}{E^* E_1 + 1} \quad i = 2, E^*/2 + 1 \quad (20)$$

Derivatives of constraints are

$$\frac{\partial g_j}{\partial x_j} = -\frac{h_j}{c} \quad j = 1, E^*/2 \quad (21)$$

$$0 \quad j = E^*/2 + 1, E^*$$

$$\frac{\partial g_j}{\partial x_j} = -\delta_{x_j} \quad 1/E^*/2 \quad \text{for } i = 2, E^*/2 + 1$$

$$\text{where, } h_{x1} = E^*/2 + 1 \quad j = 1, E^*$$

2.4. RESULTS AND DISCUSSION

2.4.1. RESULTS

Optimization studies have been carried out on rectangular composite plates, taking into consideration number of plies, aspect ratio and biaxial loading ratio as parameters for Kevlar/Epoxy composite whose material properties are as follows:

$$E_1 = 1.1 \times 10^4 \text{ kg/cm}^2$$

$$E_2 = 0.1 \times 10^4 \text{ kg/cm}^2$$

$$\nu_{12} = 0.3$$

$$\rho_{12} = 1.2 \times 10^2 \text{ kg/cm}^2$$

Numerical computations have been carried out on IBC 1090 computer. Results obtained for two sets of constraints considered are as follows :

3.4.1.6a)

Table 3.1 shows typical results obtained by varying number of plies. This indicates that the number of plies has no effect on maximum buckling load. Laminated plate behaves orthotropic properties at optimum design point, by orienting most of all the plies in the direction which results in maximum buckling load. However-the-less, conventional results obtained by considering higher number of plies provided some useful design informations which are discussed later in this section.

The variation of maximum buckling load with aspect ratio is shown in Table 3.2. The optimum fiber orientation increases from 0° to 90° with increasing aspect ratio for uniaxial loading. However, biaxial loading with $\alpha = \sigma_y / \sigma_x = 0.5$, the variation in fiber orientation is approximately from 0° to 62° for a change in aspect ratio from 1.5 to 4.0.

Table 3.3 shows that the buckling load decreases with increasing biaxial loading ratio. The optimum fiber orientation remains zero for a square plate. However, for rectangular plates it increases with biaxial loading ratio. Typical results for aspect ratio 1.5 are presented in this table.

3.4.1.1b)

Table 3.4 presents the optimum fiber orientation and corresponding buckling load for laminated plate, whose total thickness is constant but thickness of each ply can vary. These results indicate that the thickness of plies whose orientations are near optimum during three unconstrained minimization, blow up, this process, other plies use negligible thickness to satisfy the constraint of maximum total thickness. In general, thickness of outer most ply increases, except in cases where initial orientations of inner plies are very near to optimum, while fiber orientation of outer plies are far away.

The variation of buckling load with fiber orientation for orthotropic laminae plate is shown in Fig. 3.3. Aspect ratio of plate is 3.33 and compressive load is applied along x direction only. It is observed that for fiber orientations up to 30° , a half sine wave in x-direction and a half sine wave in y-direction is the primary mode of buckling, but for higher orientations primary mode of buckling is two half sine waves in x-direction and one half sine wave in y-direction. Fiber orientation of 30° gives maximum buckling load and the mode of buckling also changes at this orientation. Fig. 2.3 presents similar analysis for aspect ratio 3.3 and $E_y/E_x = 0.5$.

Fig. 1.4 presents variation in fiber orientation for each unconstrained optimization done during sequential optimization.

4.4.2. Effect of θ on Buckling

Fiber orientation of 45° leads to maximum buckling load for a square plate under uniaxial compression (Table 4.1). That, this will be so can be explained in the following manner.

Consider Eq. (13), which is reproduced in a dimensionless form, from Eq. (12) and (13) it is inferred that τ_{33} predominantly contributes to the buckling load. (For orthotropic case, where $b = 0$, only τ_{33} contributes to the buckling load)

$$B = \frac{12 \tau_{33} b^3}{\pi^2 E_3} = \frac{12 (a/b)^2}{\pi^2 E_3 U_{32} \{ \pi^2 + \pi^2 (a/b)^2 \}} \cdot \left[\tau_{33} + \frac{2 \tau_{12} \tau_{23} U_{11} + \tau_{22} \tau_{13}^2 + \tau_{11} \tau_{23}^2}{U_{11} \tau_{22} + U_{12}^2} \right] \quad (20)$$

where

$$U_{33} = E^3 \left[U_{11} \pi^4 + 2 U_{12} + 2 U_{22} \pi^2 \pi^2 (a/b)^2 + U_{22} \pi^4 (a/b)^4 \right] \quad (21)$$

The bending stiffness coefficient U_{11} decreases with increase in orientation from 0° to 90° . At 90° , U_{11} is

equal to U_{22} at 0° , U_{22} increases with orientation from 0° to 45° , U_{22} at 45° is equal to U_{11} at 0° . As 45° , U_{11} and U_{22} are equal. In view of this variation, one can easily verify that U_{33} is maximum in fiber orientation are at 45° in $n = 1$ and $n = 1$ is the primary mode of buckling). This substantiates the results obtained by optimization study.

It may be noted that U_{22} in the expression for U_{33} eq. (2c) is multiplied by $(a_y/b)^4$ and $2[U_{12} + 2U_{44}]$ is multiplied by $(a_y/b)^2$. If aspect ratio (a_y/b) is less than one, then contribution of U_{22} diminishes with decreasing aspect ratio and U_{11} tries to push optimum fiber orientation towards 0° , $2[U_{12} + 2U_{44}]$ and U_{22} try to hold its back, as a result the optimum fiber orientation is in between 0° and 45° . For aspect ratio greater than one U_{22} contributes positively and hence tries to pull up the fiber orientation. This results in the optimum fiber orientation between 45° and 90° . The above argument holds good if primary mode of buckling is a half sine wave in x and y -directions respectively. The change in buckling mode, changes contribution of each term in U_{33} expression which results in decrease in fiber orientation angle from 45° to 45° for higher aspect ratios.

The stresses for stresses in each stage for an orthotropic laminae plate (all plates with same fiber orientation) are discussed below.

(a) with $n = 1$, the change in the cross shape occurs,

where,

$$\sigma_x \text{ (or } \sigma_y, \sigma_z) = E_x \text{ (or } \sigma_y, \sigma_z)$$

(load applied in x-direction only)

this results in

$$\begin{aligned} & \frac{1}{2} \frac{\sigma}{E} \left[\frac{D_{11}}{1} \sigma^2 + 2(D_{12} + 2D_{66}) \sigma^2 (a/b)^2 + D_{22} (a/b)^4 \right] \\ & \frac{1}{(n+1)^2} \frac{\sigma}{E} \left[D_{22} (n+1)^4 + 2 (D_{12} + 2D_{66}) (n+1)^2 (a/b)^2 \right. \\ & \left. + D_{11} (a/b)^4 \right] \end{aligned} \quad (25)$$

Further simplification results in

$$(a/b)^4 = \frac{(2n+1)}{\left(\frac{1}{\sigma^2} - \frac{1}{(n+1)^2} \right) \frac{D_{11}}{E}} \cdot \frac{D_{22}}{D_{11}} \quad (26)$$

Eq. (26) gives the aspect ratio at which cross shape along x-direction changes. It is evident from equation (26) that the aspect ratio at which cross shape changes, depends on the material properties. For a plate of given thickness Eq. (26) can further be simplified, as,

$$(a/b)^4 = \frac{(2n+1)}{\left(\frac{1}{\sigma^2} - \frac{1}{(n+1)^2} \right) \frac{D_{11}}{E}} \cdot \frac{D_{22}}{D_{11}} \quad (27)$$

Let \bar{C}^* and \bar{C}_{12}^* represent the reduced stiffness coefficients at optimum fiber orientation, then

$$(a/b)^2 = \frac{\frac{1}{2}(\bar{C}_{11}^* - \bar{C}_{22}^*)}{\bar{C}_{12}^*} = \frac{\bar{C}_{12}^*}{\bar{C}_{22}^*} \quad (18)$$

For $n = 1$

$$(a/b)^2 = 1 - \frac{\bar{C}_{11}^*}{\bar{C}_{22}^*} \quad (19)$$

In order to obtain the aspect ratio for change in mode in x-direction at optimum fiber orientation, expression for optimum fiber orientation is derived. The condition for optimality with respect to fiber orientation is

$$\frac{\partial \bar{C}_i}{\partial \theta_i} = 0 \quad i = 1, 2$$

Reducing Eq. (10) to an orthotropic case and its differentiation results in

$$D_{11}^* x^4 + 2 (D_{12}^* + 2 D_{22}^*) x^2 (a/b)^2 + D_{22}^* (a/b)^4 = 0 \quad (20)$$

where D_{ij}^* are derivatives of bending stiffness coefficients with respect to fiber orientation, defined as below.

$$D_{ij}^* = 1/2 \sum_{k=1}^4 (C_{ij}^* - C_{k-k}^*) = \frac{C_{ij}^*}{12} - C_{ij}^* \quad (21)$$

where,

$$\begin{aligned} Q_{12}^* &= 2 V_2 \sin 3\alpha + 4 V_3 \sin 4\alpha \\ Q_{13}^* &= 4 V_3 \sin 4\alpha \\ Q_{22}^* &= 2 V_2 \sin 2\alpha + 4 V_3 \sin 4\alpha \\ Q_{33}^* &= 4 V_3 \sin 4\alpha \end{aligned} \quad (42)$$

V_2 and V_3 are defined as

$$\begin{aligned} V_2 &= \frac{Q_{11} - Q_{22}}{2} \\ V_3 &= \frac{Q_{11} + Q_{22} - Q_{33} - Q_{12}}{2} \end{aligned} \quad (43)$$

Substituting Eq. (42) in Eq. (40) and after simplification it yields,

$$\begin{aligned} (V_2 \sin 2\alpha^* + 2 V_3 \sin 4\alpha^*) (a_1/b)^2 + 12 V_3 \sin 4\alpha^* \\ (a_1/b)^2 = (V_2 \sin 2\alpha^* + 2 V_3 \sin 4\alpha^*) (a_1/b)^2 + 0 \end{aligned} \quad (44)$$

Eq. (44) gives the value of optimum fiber orientation for a given aspect ratio. To verify qualitative arguments given earlier, substitute $a_1/b = 1$ in Eq. (44). It results in ,

$$\sin 4\alpha^* = 0$$

and hence for maximum $a_1/b = 1$ or $a_1/b = \pi/4$ (45)

For $a_1/b = 1.25$ (Fig. 3.22) solving Eq. (66) by trial and error procedure, the aspect ratio is obtained,

$$a_2/b = 10.1 \quad (\text{Table 3.2})$$

Solving Eq. (67) for this optimum fiber orientation the aspect ratio turns out to be 1.25 for a change in mode shape along x-direction (red to 2). It shows that change in mode shape occurs at optimum.

For $n = 1$, proceeding in a similar way, the following equations are obtained,

$$(a_2/b)^2 = \frac{(2a_1 + 2)}{(2a_1^2 + 2a_1 + 2a_1 + 1)} = \frac{2C_{12}^x + 2C_{22}^x}{C_{22}^x} \quad (68)$$

or,

$$(a_2/b)^2 = \frac{(2(2a_1 + 2))}{(2a_1^2 + 2a_1 + 2a_1 + 1)} = \frac{2C_{12}^x + 2C_{22}^x}{C_{22}^x} \quad (69)$$

for $n = 1$

$$(a_2/b)^2 = \frac{2}{3} = \frac{C_{12}^x + 2C_{22}^x}{C_{22}^x} \quad (70)$$

For biaxial loading, the aspect ratio at which the mode of buckling changes, becomes a complex function of material stiffness and kind of fiber orientations. For $n = 1$, Eq. (68) defines aspect ratio for which mode of buckling changes from n to $(n+1)$ and is given below by

$$\langle \epsilon_{\theta} \epsilon_{\theta} \rangle^2 = \frac{K^2 \tau_{11}^2 (4m^2 + 6m^2 + 4m + 1)^2}{2}$$

$$\sqrt{\frac{\tau_{11}^2 (4m^2 + 6m^2 + 4m + 1)^2 + 4m^2 (2m^2 + 3m^2 + 4m + 1)}{(2m + 1) \langle \tau_{22} - 2K \langle \tau_{12} + 2 \epsilon_{22} \rangle \epsilon_{12} \rangle^2}} \quad (49)$$

$$16m - 11 \quad \tau_{22} - 2K \langle \tau_{12} + 2 \epsilon_{22} \rangle$$

Fig. 2.3 shows that crossing of mod. 1.2 and mod. 1.4 occurs at an orientation $\theta^* = 10^\circ$ which gives the maximum buckling load. This is plotted for an aspect ratio 0.5 and $K = 1.3$.

Table 2.2 reveals that fiber orientation of plies near mid-plies do not contribute much to maximum buckling load. It has been shown earlier that τ_{33} contributes predominantly to buckling load and it contains bending stiffness contributions. If τ_{13} is same for all the plies then the outer-most ply contributes maximum to τ_{13} . $\langle \epsilon_{\theta}^2 \rangle = \langle \epsilon_{\theta-1}^2 \rangle$ is maximum for outer ply due to which τ_{33} is maximum, which gives the maximum buckling load. Derivatives with respect to fiber orientations are also in line with above results. Fig. 2.4 shows that fiber orientation of outer plies reaches optimum first and fiber orientation of plies near midplane approaches optimum slowly. The latter may separate before reaching optimum orientations without making much difference in maximum buckling load.

can be applied to a two-ply plate to obtain optimum orientation. The results obtained by doing so can be used to design a plate of given aspect ratio for similar loading by varying the total thickness of plate which can be made up with plies of given thickness with optimum fiber orientations.

- (3) The designer of a composite plate for maximum buckling load can work with relax manufacturing tolerances as far as plies near the mid-plane are concerned.
- (4) In general, optimum fiber orientation is such that, slight change in orientation changes primary mode of buckling : If a designer is interested in the mode of failure, he can choose fiber orientation slightly away from the optimum to ensure particular mode without any significant change in maximum buckling load. Any fiber orientation between 40° and 50° will result in almost maximum buckling load with associated mode 1:1 for a plate of aspect ratio 1.25 (Fig. 2.2). Fiber orientation between 10° and 15° will result in maximum buckling load with associated mode 1:1 for a plate of aspect ratio 2.5 and biaxial loading ratio 0.5 (Fig. 2.3).

Table 3.1. Effect of alloying by Cu-2 on α -Fe-1000 (wt.%) (200°C)

Ingot number	Ingot wt. % Cu-20	$\frac{1}{\rho}$ $\frac{1}{\rho_0}$	(Optimum Heat treatment (hours))						Inherent strength tensile σ	Index of improvement
			$\frac{1}{\rho}$	$\frac{1}{\rho_0}$	$\frac{1}{\rho}$	$\frac{1}{\rho_0}$	$\frac{1}{\rho}$	$\frac{1}{\rho_0}$		
2	1.0	0.0	45.0	45.0					21,077	1.1
3	1.0	0.0	44.8	46.0	44.8				21,077	1.1
			45.0	45.0	45.0				21,077	1.1
4	1.0	0.0	45.0	45.0	43.8	45.4			21,076	1.1
			45.0	45.0	45.0	45.0			21,075	1.1
5	1.0	0.0	44.0	45.4	45.0	45.4	45.0		21,065	1.1
			45.0	45.0	45.0	45.0	45.0		21,073	1.1

[illegible][illegible]

TABLE 2.3. SUMMARY OF INITIAL PROPERTIES AND HIGH TEMPERATURE BEHAVIOR

No. of plates	Reinforced ratio (%/10)	$\frac{E}{E_c}$	Optimum fiber reinforcement						Reduced initial load P	Time of burning
			α_1	α_2	α_3	α_4	α_5	α_6		
6	1.0	0.0	49.3	45.6	46.5	45.5	49.3	49.3	21,913	1 h
		0.5	47.3	45.1	48.3	46.8	41.0	49.3	14,641	1 h
		—	—	—	—	—	—	—	—	—
	2.0	0.0	45.0	45.0	44.0	44.8	46.0	46.0	21,913	3 h
		0.5	43.5	41.8	47.0	46.7	43.0	44.8	12,736	2 h
		2.0	38.5	40.4	47.5	43.3	41.1	44.1	8,104	1 h
—	—	—	34.8	40.0	45.0	46.0	43.0	40.0	9,000	2 h
		—	35.8	35.0	45.0	43.8	43.0	39.0	7,500	2 h

Notes: 1. E_c = Modulus of elasticity of concrete.
2. E = Modulus of elasticity of reinforced concrete.
3. α_i = Coefficient of thermal expansion of concrete.

1998, 1999, 2000, 2001, 2002, 2003, 2004, 2005, 2006, 2007, 2008, 2009, 2010, 2011, 2012, 2013, 2014, 2015, 2016, 2017, 2018, 2019, 2020, 2021, 2022, 2023, 2024, 2025, 2026, 2027, 2028, 2029, 2030, 2031, 2032, 2033, 2034, 2035, 2036, 2037, 2038, 2039, 2040, 2041, 2042, 2043, 2044, 2045, 2046, 2047, 2048, 2049, 2050, 2051, 2052, 2053, 2054, 2055, 2056, 2057, 2058, 2059, 2060, 2061, 2062, 2063, 2064, 2065, 2066, 2067, 2068, 2069, 2070, 2071, 2072, 2073, 2074, 2075, 2076, 2077, 2078, 2079, 2080, 2081, 2082, 2083, 2084, 2085, 2086, 2087, 2088, 2089, 2090, 2091, 2092, 2093, 2094, 2095, 2096, 2097, 2098, 2099, 2100, 2101, 2102, 2103, 2104, 2105, 2106, 2107, 2108, 2109, 2110, 2111, 2112, 2113, 2114, 2115, 2116, 2117, 2118, 2119, 2120, 2121, 2122, 2123, 2124, 2125, 2126, 2127, 2128, 2129, 2130, 2131, 2132, 2133, 2134, 2135, 2136, 2137, 2138, 2139, 2140, 2141, 2142, 2143, 2144, 2145, 2146, 2147, 2148, 2149, 2150, 2151, 2152, 2153, 2154, 2155, 2156, 2157, 2158, 2159, 2160, 2161, 2162, 2163, 2164, 2165, 2166, 2167, 2168, 2169, 2170, 2171, 2172, 2173, 2174, 2175, 2176, 2177, 2178, 2179, 2180, 2181, 2182, 2183, 2184, 2185, 2186, 2187, 2188, 2189, 2190, 2191, 2192, 2193, 2194, 2195, 2196, 2197, 2198, 2199, 2200, 2201, 2202, 2203, 2204, 2205, 2206, 2207, 2208, 2209, 2210, 2211, 2212, 2213, 2214, 2215, 2216, 2217, 2218, 2219, 2220, 2221, 2222, 2223, 2224, 2225, 2226, 2227, 2228, 2229, 2230, 2231, 2232, 2233, 2234, 2235, 2236, 2237, 2238, 2239, 2240, 2241, 2242, 2243, 2244, 2245, 2246, 2247, 2248, 2249, 2250, 2251, 2252, 2253, 2254, 2255, 2256, 2257, 2258, 2259, 2260, 2261, 2262, 2263, 2264, 2265, 2266, 2267, 2268, 2269, 2270, 2271, 2272, 2273, 2274, 2275, 2276, 2277, 2278, 2279, 2280, 2281, 2282, 2283, 2284, 2285, 2286, 2287, 2288, 2289, 2290, 2291, 2292, 2293, 2294, 2295, 2296, 2297, 2298, 2299, 2300, 2301, 2302, 2303, 2304, 2305, 2306, 2307, 2308, 2309, 2310, 2311, 2312, 2313, 2314, 2315, 2316, 2317, 2318, 2319, 2320, 2321, 2322, 2323, 2324, 2325, 2326, 2327, 2328, 2329, 2330, 2331, 2332, 2333, 2334, 2335, 2336, 2337, 2338, 2339, 2340, 2341, 2342, 2343, 2344, 2345, 2346, 2347, 2348, 2349, 2350, 2351, 2352, 2353, 2354, 2355, 2356, 2357, 2358, 2359, 2360, 2361, 2362, 2363, 2364, 2365, 2366, 2367, 2368, 2369, 2370, 2371, 2372, 2373, 2374, 2375, 2376, 2377, 2378, 2379, 2380, 2381, 2382, 2383, 2384, 2385, 2386, 2387, 2388, 2389, 2390, 2391, 2392, 2393, 2394, 2395, 2396, 2397, 2398, 2399, 2400, 2401, 2402, 2403, 2404, 2405, 2406, 2407, 2408, 2409, 2410, 2411, 2412, 2413, 2414, 2415, 2416, 2417, 2418, 2419, 2420, 2421, 2422, 2423, 2424, 2425, 2426, 2427, 2428, 2429, 2430, 2431, 2432, 2433, 2434, 2435, 2436, 2437, 2438, 2439, 2440, 2441, 2442, 2443, 2444, 2445, 2446, 2447, 2448, 2449, 2450, 2451, 2452, 2453, 2454, 2455, 2456, 2457, 2458, 2459, 2460, 2461, 2462, 2463, 2464, 2465, 2466, 2467, 2468, 2469, 2470, 2471, 2472, 2473, 2474, 2475, 2476, 2477, 2478, 2479, 2480, 2481, 2482, 2483, 2484, 2485, 2486, 2487, 2488, 2489, 2490, 2491, 2492, 2493, 2494, 2495, 2496, 2497, 2498, 2499, 2500, 2501, 2502, 2503, 2504, 2505, 2506, 2507, 2508, 2509, 2510, 2511, 2512, 2513, 2514, 2515, 2516, 2517, 2518, 2519, 2520, 2521, 2522, 2523, 2524, 2525, 2526, 2527, 2528, 2529, 2530, 2531, 2532, 2533, 2534, 2535, 2536, 2537, 2538, 2539, 2540, 2541, 2542, 2543, 2544, 2545, 2546, 2547, 2548, 2549, 2550, 2551, 2552, 2553, 2554, 2555, 2556, 2557, 2558, 2559, 2560, 2561, 2562, 2563, 2564, 2565, 2566, 2567, 2568, 2569, 2570, 2571, 2572, 2573, 2574, 2575, 2576, 2577, 2578, 2579, 2580, 2581, 2582, 2583, 2584, 2585, 2586, 2587, 2588, 2589, 2590, 2591, 2592, 2593, 2594, 2595, 2596, 2597, 2598, 2599, 2600, 2601, 2602, 2603, 2604, 2605, 2606, 2607, 2608, 2609, 2610, 2611, 2612, 2613, 2614, 2615, 2616, 2617, 2618, 2619, 2620, 2621, 2622, 2623, 2624, 2625, 2626, 2627, 2628, 2629, 2630, 2631, 2632, 2633, 2634, 2635, 2636, 2637, 2638, 2639, 2640, 2641, 2642, 2643, 2644, 2645, 2646, 2647, 2648, 2649, 2650, 2651, 2652, 2653, 2654, 2655, 2656, 2657, 2658, 2659, 2660, 2661, 2662, 2663, 2664, 2665, 2666, 2667, 2668, 2669, 2670, 2671, 2672, 2673, 2674, 2675, 2676, 2677, 2678, 2679, 26

1000

[illegible]

2000-01-15
 2000-01-15
 2000-01-15
 2000-01-15

Table 2.4. (continued)

Adjusted entry λ	λ	Optimal Values						Reduced cost, Unit level μ	Remarks	
		γ_{101}	γ_{102}	γ_{201}	γ_{202}	γ_{301}	γ_{302}			
1.25	0.0	-20.5	-25.4	-25.3	-28.3	-25.4	-20.5	23.025	order 1st	
		50.0	50.0	50.0	50.0	50.0	50.0			
		-20.5	-25.4	-25.3	-28.4	-28.4	-25.4	22.72		
		50.0	50.0	51.0	51.0	51.0	51.0	23.116		
0.5	0.0	0.0	0.54	0.13	0.06	0.5	0.57	26.23	order 1st	
		21.5	15.3	50.8	73.0	66.5	35.0			
		-25	-105	0.0	-87	0.0	-56	26.05		
		12.0	15.3	22.2	79.4	16.7	11.1			
		-20.7	-20.1	-20.5	-28.1	-28.1	-20.7	21.001		
		0.5	0.7	5.9	30.0	6.6	9.4			
								27.024		
								27.024		

Table A.1. Quantities

Input ratio	$\frac{Y}{X}$	Output values						Marginal Product of L	Labor cost
		Y/Y_0	X/X_0	Y/X	Y/Y_0	X/X_0	Y/X		
2.0	0.5	1.75	0.40	4.38	0.00	-0.40	1.75	12.072	1.0000 for $H=1$
		20.00	15.50	26.47	20.00	20.00	20.00	12.000	
		100.0	10.00	10.00	100.0	100.0	10.00	12.000	
2.0	1.0	0.40	0.30	1.33	-0.25	0.14	0.50	8.000	0.0000 for $H=1$
		71.95	72.00	-0.00	45.30	72.00	71.90	0.0000	
		100.0	13.00	27.69	21.30	26.00	71.90	0.0000	

Notes:



Fig. 1.1(a) - Coordinate System & fibre orientation.

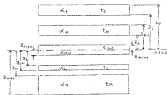


Fig.1.1. (b) - Stacking sequence & co-ordinate system for the layered plate.

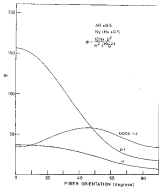


FIG. 1-3 VARIATION OF BUCKLING LOAD WITH FIBER ORIENTATION

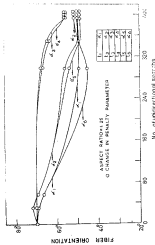


FIG. 2.4 CHANGE IN FIBER ORIENTATION DURING OPTIMIZATION

OPTIMUM WEIGHT DESIGN OF COMPOSITE PLATE UNDERIN-PLANE AND TRANSVERSE LOADING3.1 INTRODUCTION

Minimum structural weight has been considered as an important optimizables structural design in aerospace engineering applications. The advantages of composites are that they exhibit higher strength to weight ratios than metals, and have better fatigue and corrosion properties. These desirable features have resulted in an increasing use of composites in aerospace structures. Weight saving by replacing metal by composites could lead to considerable fuel saving. Besides minimum weight requirement, aircraft structures are often designed for stiffness, strength, low deflection and high buckling loads.

In chapter 2, an optimum design of composite plates to withstand various in-plane compressive loads was discussed. In this chapter, an optimum weight design of composite plates is carried out. The composite plate is subjected to requirements on deflection under transverse loading, and high buckling strength under inplane compressive loads. The study is carried out for following cases :

- (i) Optimisation of weight of a composite plate under a low deflection requirement.
- (ii) Optimisation of weight of composite plate under a high buckling load requirement and minimum deflection.

The first case is considered to understand the behaviour of deflection requirements under transverse loading. Behaviour of a plate under compressive loads is independently studied in chapter 3. Stresses in plies remain within ultimate value for all fibre orientations and hence constraints on stresses are deleted during the optimisation procedure, and an analysis is carried out at the optimum point.

2.1.1 Problem Formulation

Weight per unit area (per unit density of composite material) is optimised to facilitate a parametric study.

$$\text{Min } W' \Rightarrow \text{Min } \sum_{i=1}^N t_i \quad (2.1)$$

where $W' = \sum_{i=1}^N$

such that

$$0 \leq \theta_i \leq \pi/2 \quad ; \quad t_i \geq 0 \quad i=1, N$$

$$\omega \leq \omega^*$$

$$u_{,x} = 0, \quad v_{,x} = 0$$

Constraints are suitably modified to fit into the interior penalty function formulation. An expression for buckling load is obtained in chapter 2 (Eq. (16)). In the following sections, expressions for maximum deflection and stresses are obtained.

2.1.1.4.2.2.2

The governing Equations (5.6 and 7) remain unchanged except the term $(R_x v_{xx} + R_y v_{yy})$ is replaced by $-q$, the intensity of applied transverse load, in Eq. (7).

$$\begin{aligned} D_{11} v_{xxxx} &+ 2(D_{12} + 2D_{66}) u_{xxyy} + D_{22} v_{yyyy} \\ &- D_{11} v_{xx} - (D_{12} + 2D_{66}) u_{yy} - (D_{12} + 2D_{66}) v_{xx} \\ &- D_{22} v_{yy} = q \end{aligned}$$

The deflection of the simply supported plate is obtained by substituting Eq. (9) in Eqs. (5.6 and 7) accordingly.

$$\begin{bmatrix} -\frac{\pi^4}{a^4} & -\frac{\pi^4}{a^4} & \frac{\pi^4}{a^4} \\ \frac{\pi^4}{a^4} & -\frac{\pi^4}{a^4} & \frac{\pi^4}{a^4} \\ -\frac{\pi^4}{a^4} & -\frac{\pi^4}{a^4} & \frac{\pi^4}{a^4} \end{bmatrix} \begin{Bmatrix} \left\{ \frac{q_{mn}}{a^4} \right\} \\ \left\{ \frac{q_{mn}}{a^4} \right\} \\ \left\{ \frac{q_{mn}}{a^4} \right\} \end{Bmatrix} = \begin{Bmatrix} 0 \\ 0 \\ q_{mn} \end{Bmatrix} \quad (5a)$$

$$\text{where } q = \sum \sum q_{mn} \sin \frac{n\pi x}{a} \sin \frac{m\pi y}{b}$$

and τ_{ij} are as defined in Eq. (11)

q_{mn} for uniform loading is,

$$q_{mn} = \frac{16 q_0}{\pi^2} \frac{1}{m^2} \frac{1}{n^2} \quad \begin{matrix} m = 1, 3, 5, \dots \\ n = 1, 3, 5, \dots \end{matrix} \quad (12)$$

where

q_0 = applied uniform loading per unit area
Eq. (12) is solved using Green's eqn. and following
expressions are obtained.

$$\begin{aligned} q_{mn} &= \frac{q_0}{\pi^2} \frac{1}{m^2} (\tau_{22} \tau_{11} - \tau_{12} \tau_{21}) \\ q_{mn} &= \frac{q_0}{\pi^2} \frac{1}{n^2} (\tau_{11} \tau_{22} - \tau_{12} \tau_{21}) \end{aligned} \quad (13)$$

and

$$q_{mn} = \frac{q_0}{\pi^2} \frac{1}{m^2} (\tau_{22} \tau_{11} - \tau_{12}^2)$$

where

$$\begin{aligned} D &= \frac{(\tau_{11} \tau_{22} - \tau_{12}^2)}{a^2} \left[\tau_{11} + \right. \\ &\quad \left. \frac{2 \tau_{12} \tau_{13} \tau_{23} - \tau_{22} \tau_{13}^2 - \tau_{11} \tau_{23}^2}{\tau_{11} \tau_{22} - \tau_{12}^2} \right] \end{aligned}$$

Knowing deformations, the maximum strain in a lamina can be obtained in the following manner

$$\begin{aligned}\epsilon_x &= u_x = \frac{\partial u}{\partial x} \\ \epsilon_y &= v_y = \frac{\partial v}{\partial y} \\ \epsilon_{xy} &= u_y = v_x = \frac{\partial u}{\partial y} = \frac{\partial v}{\partial x}\end{aligned}\quad (34)$$

where u and v are the in-plane deflections at the selected surface, which is mid-surface in our case, since the reference surface deflections u and v , the plate curvatures w_{xx} and w_{yy} , and the plate twist w_{xy} are all included in any given point in the plate, the stresses at the surface x in the k^{th} lamina are given by

$$\begin{Bmatrix} \sigma_x^{(k)} \\ \sigma_y^{(k)} \\ \sigma_{xy}^{(k)} \end{Bmatrix} = \begin{bmatrix} Q_{11}^{(k)} & Q_{12}^{(k)} & Q_{13}^{(k)} \\ Q_{21}^{(k)} & Q_{22}^{(k)} & Q_{23}^{(k)} \\ Q_{31}^{(k)} & Q_{32}^{(k)} & Q_{33}^{(k)} \end{bmatrix} \begin{Bmatrix} \epsilon_x^{(k)} \\ \epsilon_y^{(k)} \\ \epsilon_{xy}^{(k)} \end{Bmatrix} \quad (35)$$

3.2.2 DERIVATIVES OF STRESS AND TRANSVERSE DEFLECTION

The optimization algorithm requires the derivatives of stresses and transverse deflection. These are obtained as follows.

Let x_i be design variables $i = 1, 2$
 For the present case,

$$x_1 = x_1 \quad i = 1, 2^{1/2}$$

$$\text{and} \quad x_2 = x_2 \quad i = 2^{1/2} = 1, 2^2$$

substituting Eq. (11) in Eq. (4) and differentiating, following conditions are obtained,

$$\frac{\partial f_1}{\partial x_1} = \frac{\partial f_1}{\partial x_1} \left[\frac{\partial_1 \frac{\partial^2 f_1}{\partial x_1^2} x_{23} + \frac{\partial_1 \frac{\partial^2 f_1}{\partial x_1^2}}{2^2} \right]$$

$$\frac{\partial^2 f_1}{\partial x_1^2} x_{12} = \frac{\partial^2 f_1}{\partial x_1^2} x_{23} = \frac{\partial^2 f_1}{\partial x_1^2} x_{23} = \frac{\partial^2 f_1}{\partial x_1^2} x_{23} = \frac{\partial^2 f_1}{\partial x_1^2} x_{23}$$

$$\cos (n \pi y/a) \sin (n \pi x/b) \quad (16)$$

$$\frac{\partial f_1}{\partial x_1} = \frac{\partial f_1}{\partial x_1} \left[\frac{\partial_1 \frac{\partial^2 f_1}{\partial x_1^2} x_{23} + \frac{\partial_1 \frac{\partial^2 f_1}{\partial x_1^2}}{2^2} \right]$$

$$\frac{\partial^2 f_1}{\partial x_1^2} x_{12} = \frac{\partial^2 f_1}{\partial x_1^2} x_{23} = \frac{\partial^2 f_1}{\partial x_1^2} x_{23} = \frac{\partial^2 f_1}{\partial x_1^2} x_{23} \quad (17)$$

$$\sin (n \pi y/a) \cos (n \pi x/b)$$

Let v_i be design variables $i = 1, 1'$

For the present case,

$$v_1 = v_2 \quad i = 1, \beta'/\beta$$

$$\text{and} \quad v_1 = v_2 \quad i = \alpha'/\alpha = 1, \alpha'$$

Substituting Eq. (53) in Eq. (4) and differentiating, following relations are obtained,

$$\frac{\partial v_1}{\partial v_2} = \frac{v_1}{v_2} \left(\frac{\partial \left(\frac{\partial}{\partial v_1} v_{12} \right)}{\frac{\partial}{\partial v_1} v_{12}} + \frac{\partial \left(\frac{\partial}{\partial v_2} v_{12} \right)}{\frac{\partial}{\partial v_2} v_{12}} \right) =$$

$$\left(\frac{\frac{\partial}{\partial v_1} v_{12}}{\frac{\partial}{\partial v_1} v_{12}} + \frac{\frac{\partial}{\partial v_2} v_{12}}{\frac{\partial}{\partial v_2} v_{12}} \right) \left(\frac{\partial}{\partial v_1} v_{12} \right) = \frac{\partial}{\partial v_1} v_{12} + \frac{\partial}{\partial v_2} v_{12} \left(\frac{\partial}{\partial v_2} v_{12} \right) \left(\frac{\partial}{\partial v_1} v_{12} \right)$$

$$\sin (\alpha' \pi / \alpha) \sin (\alpha' \pi / \alpha) \quad (54)$$

$$\frac{\partial v_1}{\partial v_2} = \frac{v_1}{v_2} \left(\frac{\partial \left(\frac{\partial}{\partial v_1} v_{12} \right)}{\frac{\partial}{\partial v_1} v_{12}} + \frac{\partial \left(\frac{\partial}{\partial v_2} v_{12} \right)}{\frac{\partial}{\partial v_2} v_{12}} \right) =$$

$$\left(\frac{\frac{\partial}{\partial v_1} v_{12}}{\frac{\partial}{\partial v_1} v_{12}} + \frac{\frac{\partial}{\partial v_2} v_{12}}{\frac{\partial}{\partial v_2} v_{12}} \right) \left(\frac{\partial}{\partial v_1} v_{12} \right) = \frac{\partial}{\partial v_1} v_{12} + \frac{\partial}{\partial v_2} v_{12} \left(\frac{\partial}{\partial v_2} v_{12} \right) \left(\frac{\partial}{\partial v_1} v_{12} \right) \quad (55)$$

$$\sin (\alpha' \pi / \alpha) \sin (\alpha' \pi / \alpha)$$

$$\frac{\partial \bar{u}}{\partial v_1} = \frac{5\pi^2}{8} \left[\frac{\left(\frac{\partial^2 \tau_{12}}{\partial v_1^2} + \tau_{11} + \tau_{22} \frac{\partial^2 \tau_{11}}{\partial v_1^2} - 2\tau_{12} \frac{\partial^2 \tau_{12}}{\partial v_1^2} \right)}{\delta^2} - (\tau_{22} \tau_{11} - \tau_{12}^2) \frac{\partial \delta}{\partial v_1} \right] \quad (54)$$

where

$$\begin{aligned} \frac{\partial \delta}{\partial v_1} &= \frac{1}{\delta} \left(\frac{\partial^2 \tau_{12}}{\partial v_1^2} \tau_{12} + \tau_{11} \frac{\partial^2 \tau_{22}}{\partial v_1^2} - 2\tau_{12} \frac{\partial^2 \tau_{12}}{\partial v_1^2} \right) \\ &\quad \left[\frac{\partial^2 \tau_{12}}{\partial v_1^2} + \left\{ (\tau_{11} \tau_{22} - \tau_{12}^2) \left(2 \frac{\partial^2 \tau_{12}}{\partial v_1^2} \tau_{22} \tau_{12} + 2 \frac{\partial^2 \tau_{12}}{\partial v_1^2} \right. \right. \right. \\ &\quad \left. \left. \tau_{12} \tau_{22} + 2 \frac{\partial^2 \tau_{12}}{\partial v_1^2} \tau_{12} \tau_{22} - \frac{\partial^2 \tau_{22}}{\partial v_1^2} \tau_{12}^2 - 2 \frac{\partial^2 \tau_{12}}{\partial v_1^2} \tau_{12} \tau_{22} \right. \right. \\ &\quad \left. \left. - \frac{\partial^2 \tau_{11}}{\partial v_1^2} \tau_{22}^2 - 2 \frac{\partial^2 \tau_{22}}{\partial v_1^2} \tau_{12} \tau_{22} \right) + (2 \tau_{12}^2 \tau_{22} \tau_{12} - \tau_{22}^2 \tau_{12} \right. \\ &\quad \left. \left. - \tau_{11}^2 \tau_{22}^2) \right\} \right] \\ &\quad \left(\frac{\partial^2 \tau_{12}}{\partial v_1^2} \tau_{12} + \frac{\partial^2 \tau_{22}}{\partial v_1^2} \tau_{22} - 2 \frac{\partial^2 \tau_{12}}{\partial v_1^2} \tau_{12} \tau_{22} \right) / \\ &\quad \left(\tau_{11} \tau_{22} - \tau_{12}^2 \right)^2 \} \end{aligned}$$

and

$$\frac{\partial^2 \tau_{11}}{\partial v_1^2} \quad \text{are given by Eq. (13)}$$

Gradients of stresses can be obtained in the following manner :

$$\frac{\partial \sigma_{ij}^{(k)}}{\partial v_j} = \lambda \frac{\partial \sigma_{ij}^{(k)}}{\partial v_j} + \left[\frac{\partial \sigma_{ij}^{(k)}}{\partial v_j} \right] \frac{\partial v_j}{\partial v_j} \quad i = 1,2, \text{ and } 3 \\ i = 1,2 \text{ and } 3 \\ j = 1, 2 \quad (9.2)$$

where

$$\frac{\partial \epsilon_x}{\partial v_j} = \frac{\partial \epsilon_x}{\partial v_j} = \left[\frac{\partial \epsilon_x}{\partial v_j} \right] \frac{\partial v_j}{\partial v_j} \quad v_{xx} \\ \frac{\partial \epsilon_y}{\partial v_j} = \frac{\partial \epsilon_y}{\partial v_j} = \left[\frac{\partial \epsilon_y}{\partial v_j} \right] \frac{\partial v_j}{\partial v_j} \quad v_{yy} \\ \frac{\partial \epsilon_{xy}}{\partial v_j} = \frac{\partial \epsilon_{xy}}{\partial v_j} = \left[\frac{\partial \epsilon_{xy}}{\partial v_j} \right] \frac{\partial v_j}{\partial v_j} = 2 \left[\frac{\partial \epsilon_{xy}}{\partial v_j} \right] v_{xy}$$

Derivatives of $\{\sigma_{ij}\}$ and λ are given in Appendix - 1 .

2.2.2. CONSTRAINTS AND THEIR GRADIENTS

Constraints and their derivatives for the optimisation studies are observed as follows.

The set of constraints described by Eqs. (14-16) in chapter 1 are also applied to minimum weight

optimization problem considered here. Their derivatives are given by Eqs. (17,18 and 20). In addition to these constraints, constraints on the maximum deflection and the ultimate stresses in principal directions of Tsai - Hill yield criterion for anisotropic materials, are applied in the first problem. Second problem includes constraint on buckling in addition to the constraints imposed on the first problem.

The additional constraints are

$$g_1 = 1 - w/w^* \quad (82)$$

$$g_2 = (1/\sigma_x^* \sigma_y^*) - 1 \quad (83)$$

$$g_3 = 1 + \frac{\sigma_{xy}^* - 2}{\sigma_x^*} \quad i = 1, 2, 3 \quad (84)$$

$$g_4 = 1 - \frac{E_T (1 - (2i+1))}{G_T} \quad i = 0, 2, 3, 4 \quad (85)$$

$$g_5 = 1 - \frac{E_{22} (1 - (2i+1))}{G_{22}} \quad i = 2, 3, 4 \quad (86)$$

and

$$g_6 = 1 - \left(\frac{\sigma_{xy}^* - 2}{\sigma_x^*} \right)^2 + \frac{E_{22} (1 - (2i+1))}{G_{22}} \left(\frac{\sigma_{xy}^* - 2}{\sigma_x^*} \right) + \left(\frac{\sigma_{xy}^* - 2}{G_{22}} \right)^2 \quad i = 1, 2, 3 \quad (87)$$

where

$$\begin{Bmatrix} \sigma_x^2 \\ \sigma_y^2 \\ \sigma_{xy}^2 \end{Bmatrix} = [T]^{-1} \begin{Bmatrix} \sigma_{10}^2 \\ \sigma_{70}^2 \\ \sigma_{170}^2 \end{Bmatrix} \quad (56)$$

where

$$[T]^{-1} = [T]^T = \begin{vmatrix} \cos^2 \alpha & \sin^2 \alpha & -2 \sin \alpha \cos \alpha \\ \sin^2 \alpha & \cos^2 \alpha & +2 \sin \alpha \cos \alpha \\ 2 \sin \alpha \cos \alpha & -2 \sin \alpha \cos \alpha & \cos^2 \alpha - \sin^2 \alpha \end{vmatrix} \quad (57)$$

It should be noted that the fiber at orientations $+\alpha$ and $-\alpha$ will contribute to the ultimate strength in the principal directions, therefore,

$$\begin{aligned} \sigma_x^2 &= \sigma_{10}^2 \sin^2 \alpha + \sigma_{70}^2 \cos^2 \alpha \\ \sigma_y^2 &= \sigma_{10}^2 \sin^2 \alpha + \sigma_{70}^2 \cos^2 \alpha \\ \sigma_{xy}^2 &= \sigma_{170}^2 (\cos^2 \alpha - \sin^2 \alpha) \end{aligned} \quad (58)$$

Derivatives of constraints are

$$\frac{\partial \sigma_1}{\partial \sigma_1^2} = - \frac{1}{\sigma_1^2} \frac{\partial \sigma_1}{\partial \sigma_1^2} \quad i = 1, 2 \quad (59)$$

$$\frac{\partial \sigma_2}{\partial \sigma_1^2} = - \frac{1}{\sigma_2^2} \frac{\partial \sigma_2}{\partial \sigma_1^2} \quad i = 1, 2 \quad (60)$$

$$\frac{\partial v_j}{\partial v_j} = - \frac{1}{\sigma} \frac{\partial \sigma_{xj+2}}{\partial v_j} \quad \begin{matrix} l=3, 3+2 \\ j=1, 3'' \end{matrix} \quad (73)$$

$$\frac{\partial v_j}{\partial v_j} = - \frac{1}{\sigma} \frac{\partial \sigma_{xj+2-2(2+2)}}{\partial v_j} \quad \begin{matrix} l=3+2, 3+2 \\ j=1, 3'' \end{matrix} \quad (74)$$

$$\frac{\partial v_j}{\partial v_j} = - \frac{1}{\sigma} \frac{\partial \sigma_{xj+2-2(2+2)}}{\partial v_j} \quad \begin{matrix} l=3+2, 3+2 \\ j=1, 3'' \end{matrix} \quad (75)$$

or

$$\begin{aligned} \frac{\partial v_j}{\partial v_j} = & - \frac{\sigma_{xj+2}}{\sigma^2} \frac{\partial \sigma_{xj+2}}{\partial v_j} + \frac{\sigma_{xj+2}}{\sigma^2} \frac{\partial \sigma_{xj+2}}{\partial v_j} \\ & + \frac{\sigma_{xj+2}}{\sigma^2} \frac{\partial \sigma_{xj+2}}{\partial v_j} - \frac{\sigma_{xj+2}}{\sigma^2} \frac{\partial \sigma_{xj+2}}{\partial v_j} \end{aligned}$$

$$\begin{matrix} l = 3, 3+2 \\ j = 1, 3'' \end{matrix} \quad (76)$$

1.4. ANALYSIS AND DISCUSSION

1.4.1. ANALYSIS

Minimum weight optimisation of a rectangular plate has been carried out for varying grades of plates and aspect ratios, for Kevlar/epoxy composite, whose material properties are as given in section(2.4.1),

$$\frac{\partial \sigma_j}{\partial v_j} = - \frac{1}{2} \frac{\partial \sigma_{j-1,j}}{\partial v_j} \quad 1 \leq j, n+2 \\ j=1, 2^n \quad (73)$$

$$\frac{\partial \sigma_j}{\partial v_j} = - \frac{1}{2} \frac{\partial \sigma_{j-1,j} \partial \sigma_{j+1,j}}{\partial v_j} \quad 1 \leq j \leq n, n+1 \\ j=1, 2^n \quad (74)$$

$$\frac{\partial \sigma_j}{\partial v_j} = - \frac{1}{2\gamma} \frac{\partial \sigma_{j-1,j} \partial \sigma_{j+1,j}}{\partial v_j} \quad 1 \leq j \leq n, n+1 \\ j=1, 2^n \quad (75)$$

and

$$\begin{aligned} \frac{\partial \sigma_j}{\partial v_j} = - & \frac{\sigma_{j-1,j}}{x_j^2} \frac{\partial \sigma_{j-1,j}}{\partial v_j} + \frac{\sigma_{j+1,j}}{x_j^2} \frac{\partial \sigma_{j+1,j}}{\partial v_j} \\ & + \frac{\sigma_{j-1,j}}{\sigma_j^2} \frac{\partial \sigma_{j-1,j}}{\partial v_j} - \frac{\sigma_{j+1,j}}{\sigma_j^2} \frac{\partial \sigma_{j+1,j}}{\partial v_j} \\ & 1 = 2, n+1 \\ & 1 = 1, 2^n \end{aligned} \quad (76)$$

3.4. RESULTS AND DISCUSSION

3.4.1. RESULTS

Minimum weight optimization of a four-layered plate has been carried out for various number of plies and aspect ratios, for Kevlar/epoxy composite. Above material properties are as given in section(3.4.1).

Numerical results have been computed for the following set of constraints :

Longitudinal tensile strength	= 140.37 kg/sq.cm.
Transverse tensile strength	= 8.43 kg/sq.cm.
Longitudinal compressive strength	= 202.13 kg/sq.cm.
Transverse compressive strength	= 28.11 kg/sq.cm.
Shear strength	= 11.65 kg./sq.cm.
Applied uniform transverse loading	= 0.0025 kg/sq.cm.
Upper limit on maximum deflection	= 1.00 mm.
Minimum buckling load in x-direction	= 0.00 kg/cm.

Table 3.1 presents the optimum ply thickness and corresponding fiber orientation for a minimum weight design of a plate subjected to uniform transverse loading. The deflection of the plate is restricted to be within prescribed upper limit. Results for different aspect ratios are tabulated. For each aspect ratio, a plate with varying number of plies is considered.

The variation of the maximum deflection with fiber orientation is plotted in Fig. 3.1. The minimum of the maximum deflection of the plate is obtained at

highest fiber orientations as aspect ratio increases. The change in maximum deflection is small for plates of low aspect ratio while for plates of higher aspect ratios, it increases rapidly.

Figs. (3.2.3.3 and 3.4) show the variations of stresses in positive fiber direction, transverse to fiber direction, and shear stress with fiber orientation, respectively.

The optimum ply thickness and corresponding fiber orientations for plates with varying aspect ratio and biaxial loading ratio are presented in Table 3.1. Optimum fiber orientation angle increases with an increase in biaxial loading ratio for lower aspect ratios. The change is small as aspect ratio approaches unity. For a square plate the fiber orientation angle remains constant (45°) with increase in biaxial loading ratio. The contribution of plate thickness near mid-span is not considerable. In fact, the fiber orientation of the glass near mid-span do not achieve an optimum orientation, but their effect is nullified, as a result, by reducing the thickness to an almost negligible value.

Fig. 3.6 shows the variation of the optimum weight with aspect ratio for different lateral loading ratios. The optimum weight is higher for higher lateral loading ratios. But at higher aspect ratios it remains unchanged with varying lateral loading ratio. The maximum deflection and buckling load are plotted against aspect ratio in Fig. 3.8. The figure shows the active constraint for a given aspect ratio and lateral loading, and it also represents the value of the other constraint for the ratio.

Fig. 3.7 presents the optimum weights for a given lateral loading, for plates with different aspect ratios. The optimum weight remains unchanged for higher aspect ratios at lower lateral loading ratios.

3.4. VARIATION OF ASPECT

In previous, a designer would be interested in knowing how the response quantities vary with a change in the design variable. In chapter 2, an attempt was made to understand the effect of stability criterion on the optimum design of the plate. In this chapter, the deflection under transverse loading is dealt with separately to facilitate the designer in visualizing the design variables, and, sometimes, to understand the behavior of the design variables near optimum value.

Eq. 3.36 is sending off the variables to the nearest physical value. Figs. (3.3-3.4) present the results of the analysis. Fig. 3.3 presents the variation of the maximum dimensional deflection of composite plate with fiber orientation. Variation of stress in positive fiber direction, stress transverse to positive fiber direction, and shear stress (σ_{xy}), with fiber orientation (cf. stress in Fig. 3.3, Fig. 3.3 and Fig. 3.4, respectively).

The requirement on deflection is very stringent in all composite designs. Lesser deflection or bending is the governing design criterion and the stresses never exceed the ultimate value if the design remains within the requirements for deflection and stability. Figs. (3.3-3.4) indicate this behavior. (Carbon filaments have a high modulus and high strength and low bending. Kevlar's strength is often designed for stiffness and compressional loads. Fiber is particularly suitable for low deflection and high strength applications.) Again, the requirement on stress or strength criterion is never closer than the optimum. These constraints are detected during optimization procedure and only analysis is done at the first optimum point.

Eq. (10) and Eq. (11) show that the factor

$$1/\pi^3 \alpha^3 \left\{ \alpha^2 + 2\alpha^2 \tan^2 \theta \right\}$$

appears in the expression for \bar{D}_x , and $\lambda^4 q_{\text{lim}}$ appears in the expressions for the transverse deflection. It means that at lower aspect ratios, buckling will be the governing criterion, while at higher aspect ratios, the deflection will be an active constraint. With higher values of lateral loading, the change-over from buckling to deflection as an active constraint will take place at still higher aspect ratios. Analysis, similar to that done in section (3.4.2) will substantiate the results obtained for the optimum fiber orientations in table 3.3. The reasons given for the variations of ply thickness, at the end of section (3.4.3), hold good for results presented in table 3.3 and table 3.4.

The optimum weight does not depend upon the lateral loading ratio if the constraint on deflection is active. It increases with increase in lateral loading ratio because the buckling load decreases with increasing lateral loading ratio and, hence, the thickness of the laminate has to compensate for it to get the design to satisfy the stability requirement (fig. 3.7).

4. CONCLUSIONS

The following conclusions can be drawn.

- (1) The weight per unit area of the plate increases with increasing aspect ratio. However, it seems to approach an asymptotic value with aspect ratio.

- (2) Stability criterion is the active constraint at lower aspect ratios. The minimum deflection is the active constraint at higher aspect ratios.
- (3) The change from the stability criterion to the deflection criterion as an active constraint, takes place at higher aspect ratios with increase in biaxial loading.
- (4) Buckling never become active at optimum point with the low deflection requirement at the laminar design. These constraints can be selected to improve the efficiency of the algorithm.

Conclusions given at the end of chapter 2, in general, hold for the minimum weight design under structural deflection and stability constraints, too.

TABLE 2-1 - THE DESIGN VALUES OF THE 100 PROBES AND
 CORRELATION WITH TEST OBSERVATIONS FOR 10 PROBES
 (DATA OBTAINED LOCATED IN APPENDIX)

subject probe no.	No. of pilot tests	Design Values					Test values \bar{y}/σ
		\bar{y}	σ	\bar{y}/σ	\bar{y}/σ	\bar{y}/σ	
1	2	0.83	0.77				1.04
		0.31	0.21				
4	2	0.92	0.09	0.04	0.92		1.04
		0.08	20.00	10.55	0.05		
6	2	0.03	0.12	0.09	0.03	0.10	0.75
		0.10	20.11	41.06	01.00	21.00	
8	2	0.05	1.03				1.30
		23.02	13.02				
6	2	0.07	0.07	0.17	0.07		1.35
		39.02	40.02	20.07	27.02		
6	2	1.02	0.02	0.03	0.03	1.03	1.35
		39.04	01.04	40.03	01.03	39.03	

2018 U. S. Nat. Cooperator

Subject code	No. of plots	Jettison status						Upstream subject code
		χ^2_{stat}	χ^2_{crit}	χ^2_{stat}	χ^2_{crit}	χ^2_{stat}	χ^2_{crit}	
1.0	3	24.09	3.84					4.00
		45.7	45.0					
	6	1.00	1.00	3.00	1.00			4.01
		45.0	40.00	44.00	45.0			
2	3	45.0	45.0	45.0	45.0	40.0	45.0	4.01
		4.07	0.07	0.07	0.07	0.07	0.07	
	6	2.29	2.29					
3.25	3	52.07	52.00					
	6	1.50	0.72	0.72	1.14			4.50
		55.7	48.0	48.00	53.00			
6	3	0.04	0.04	0.07	0.04	0.04	0.04	
		58.06	52.00	46.00	45.00	53.12	48.12	4.51

TABLE 2.1. CONTINUED

Support radius	No. of plates	Optimum values						Optimum required width
		$V_{f/4.1}$	$V_{f/4.2}$	$V_{f/4.3}$	$V_{f/4.4}$	$V_{f/4.5}$	$V_{f/4.6}$	
2.0	2	2.52	2.37					4.02
		59.79	69.74					
4	4	2.26	0.12	4.44	2.25			4.02
		69.7	50.28	61.22	68.69			
6	6	2.17	0.15	4.43	0.12	0.15	2.17	4.02
		68.12	42.20	47.69	47.79	63.10	68.12	

TABLE 1.2. VARIATION OF OPTIMUM VALUES WITH INJECT PUMP AND STATIONARY INJECTION METHOD

Injunct method	$\frac{E}{\mu}$	Station thick	Optimum of thickness μ/m				Optimum weight $\mu/\mu A$
			T_{opt}	T_{opt}	T_{opt}	T_{opt}	
0.5	0.0	5	1.00	1.00			1.85
			0.00	0.00			
			1.00	0.00	0.00	1.00	
			0.00	0.00	0.00	0.00	
0.5	0.0	5	1.00	1.00			2.55
			0.00	0.00			
			1.00	0.00	0.00	1.00	
			0.00	0.00	0.00	0.00	
0.5	0.0	5	1.00	1.00			2.60
			0.00	0.00			
			1.00	0.00	0.00	1.00	
			0.00	0.00	0.00	0.00	
0.5	0.0	5	1.00	1.00			2.65
			0.00	0.00			
			1.00	0.00	0.00	1.00	
			0.00	0.00	0.00	0.00	
0.5	0.0	5	1.00	1.00			2.81
			0.00	0.00			
			1.00	0.00	0.00	1.00	
			0.00	0.00	0.00	0.00	
0.5	0.0	5	1.00	1.00			2.85
			0.00	0.00			
			1.00	0.00	0.00	1.00	
			0.00	0.00	0.00	0.00	

TABLE 3.2. CONTINUED

Approximate orbital radius R_p in a_J	No. of planets	Optimum dry atmosphere				Optimum surface pressure mbar
		T_{opt1}	T_{opt2}	T_{opt3}	T_{opt4}	
1.5	3	1.46	1.46			2.81
		28.12	28.12			
		1.20	0.00	0.04	1.55	
		22.1	22.9	51.0	23.8	
0.0	3	1.49	1.70			3.39
		27.8	27.45			
		1.38	0.10	0.11	1.59	
		21.03	42.47	42.29	27.03	
0.5	1	1.73	1.73			3.44
		16.00	25.79			
		2.00	0.73	0.21	1.03	
		13.35	43.34	43.38	27.9	
	2					3.68

Table 1-1. (Continued)

Aspect ratio	$\frac{b}{a}$	No. of piles	Nominal pile frictional load				Optimum bearing capacity
			C_{p1}/k	C_{p2}/k	C_{p3}/k	C_{p4}/k	Q_p/p^2
1.5		2	1.40	1.00			3.10
			38.33	28.28			
		4	1.38	.60	.65	1.34	3.70
			35.25	41.06	43.53	33.88	
3.0		2	1.06	1.06			3.83
			37.33	37.03			
		4	1.07	0.15	0.15	1.75	3.86
			37.5	43.0	43.0	33.8	
5.0		2	2.07	3.00			4.03
			48.8	48.8			
		4	1.00	1.48	2.50	1.50	4.03
			48.5	48.8	48.5	48.5	
7.0		2	2.70	2.00			4.03
			43.0	43.0			

Table 1.2. continued

Age and sex ratio	$\frac{E}{E_{\text{max}}}$	No. of pelles	Ovarian size (mm)				Ovarian weight (mg)
			$E_{\text{ov}}/E_{\text{ov}}^{\text{max}}$	$E_{\text{ov}}/E_{\text{ov}}^{\text{max}}$	$E_{\text{ov}}/E_{\text{ov}}^{\text{max}}$	$E_{\text{ov}}/E_{\text{ov}}^{\text{max}}$	
1-2	0.1	4	1.00	0.00	1.00	4.00	4.00
			0.50	0.00	0.50	0.50	
			0.00	0.00	0.00	0.00	
2-3	0.2	3	2.00	1.00	1.00	4.00	4.00
			1.50	0.50	0.50		
			0.00	0.00	0.00		
3-4	0.3	4	3.00	2.00	1.00	4.00	4.00
			2.50	1.50	0.50		
			0.00	0.00	0.00		
4-5	0.4	3	4.00	3.00	1.00	4.00	4.00
			3.50	2.50	0.50		
			0.00	0.00	0.00		
5-6	0.5	4	5.00	4.00	1.00	4.00	4.00
			4.50	3.50	0.50		
			0.00	0.00	0.00		
6-7	0.6	4	6.00	5.00	1.00	4.00	4.00
			5.50	4.50	0.50		
			0.00	0.00	0.00		
7-8	0.7	4	7.00	6.00	1.00	4.00	4.00
			6.50	5.50	0.50		
			0.00	0.00	0.00		
8-9	0.8	4	8.00	7.00	1.00	4.00	4.00
			7.50	6.50	0.50		
			0.00	0.00	0.00		
9-10	0.9	4	9.00	8.00	1.00	4.00	4.00
			8.50	7.50	0.50		
			0.00	0.00	0.00		
10-11	1.0	4	10.00	9.00	1.00	4.00	4.00
			9.50	8.50	0.50		
			0.00	0.00	0.00		

TABLE 1.2. CONTINUED

Depth below surface feet	$\frac{W}{A}$ $\frac{1}{\text{ft}^2}$	No. of plates	$V_{1/2}$	$V_{1/3}$	$V_{2/3}$	$V_{3/4}$	Optimum salinity w/pct
0.5		2	20.26	20.26			4.57
			52.8	52.8			
		1	20.26	0.52	0.57	1.10	4.57
			52.7	50.3	50.5	52.8	
1.0		2	20.26	20.26			4.57
			52.8	52.7			
		2	20.26	0.10	0.23	2.06	4.57
			52.8	49.7	49.7	52.8	
1.5		2	20.26	20.26			4.57
			52.8	52.0			
		1	19.58	0.69	0.62	1.79	4.57
			52.3	51.3	51.8	52.3	
2.0		2	20.26	20.26			4.57
			52.9	50.8			
		4	20.15	5.53	1.57	2.16	4.57
			49.9	50.4	50.3	50.9	

Table 3.4. Continued

Project Name	E_c ksi	No. of Inches	Sectional Properties				Design Weight w/p.c.
			I_{x1}	I_{x2}	I_{p0}	I_{p1}	
3.4	0.5	2	20.45	2.05			4.070
			10.0	100.0			
			0.20	0.005	0.00	21.50	3.070
		4	69.0	69.1	62.4	69.0	
3.4	0.4	2	2.00	2.01			4.00
			61.0	60.9			
			10.20	0.23	0.20	1.20	4.000
		4	45.0	50.1	54.5	69.0	
3.4	0.3	2	0.03	2.00			0.000
			70.0	70.0			
			0.15	0.00	0.00	20.00	0.000
		4	21.0	69.0	61.0	70.0	

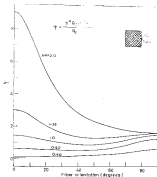


FIG. 3.1 MAXIMUM DEFLECTION OF SIMPLY SUPPORTED LAMINATED PLATE VS FIBER ORIENTATION

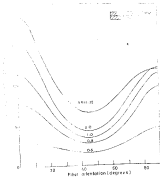


FIG. 5-7 VARIATION OF COMPRESSIVE STRESS WITH FIBER ORIENTATION

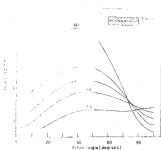


FIG. 3.1 VARIATION OF INVERSE STRESS VS FIBER ORIENTATION

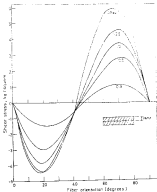


FIG. 14. VARIATION OF SHEAR STRESS WITH FIBER ORIENTATION

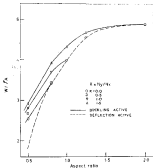


FIG. 3.6. VARIATION OF OPTIMUM WEIGHT WITH ASPECT RATIO.

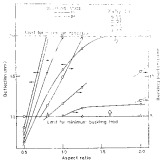


FIG. 3-8 VARIATION OF DEFLECTION AND BUCKLING LOAD WITH ASPECT RATIO FOR OPTIMUM VERTICAL OFFSET

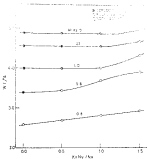


FIG. 3.7 VARIATION OF OPTIMIZATION DEPTH WITH RADIAL LOADING RATIO

OPTIMAL WEIGHT DESIGN OF THE ANISOTROPIC LAMINATE
COMPOSITE PLATE

4.1 INTRODUCTION

In the previous chapters, a laminated plate with orthotropic laminae is considered for optimal weight design. This orthotropy is achieved by embedding an equal number of fibers at positive and negative orientations with respect to the structured axis, 45° or 90° in a ply. In this chapter, another class of laminated composite plates is considered, namely, the antisymmetric angle-ply laminates. Coupling between in-plane stretching and twist exists in this case. Also, the coupling stiffness matrix elements B_{16} and B_{26} exist in this case. Sharma, et. al. (1a) have shown that this coupling can be eliminated completely or partially by choosing the thickness ratios for plies suitably. It is well known that if this coupling is reduced or eliminated, the strength of laminate increases.

Again, an attempt is made to obtain a minimum weight design for antisymmetric angle-ply laminates subjected to in-plane compressive and transverse loadings. The term antisymmetric is used in the sense that lamina thickness distributions with positive and negative fiber

orientations are located at equal intervals about the structural axis. The analysis is quite general and can be applied to any type of antisymmetric.

The following studies are conducted to each plate:

- (1) Minimum weight design of antisymmetric angle-ply laminates with variable thickness of plate. The fiber orientations are pre-assigned.
- (2) Minimum weight design of antisymmetric angle-ply laminates treating the thickness of plate and the corresponding fiber orientations as design variables.

4.2 PROBLEM FORMULATION

For these problems the objective function is

$$\min \sum_{i=1}^{N/2} t_i, \quad \text{where, } i = \text{Total no. of plates} \quad (27)$$

such that

$$-\pi/2 \leq \alpha_i \leq \pi/2, \quad i=1, N/2$$

$$t_i \leq t_j \leq t_N, \quad i=1, N/2 \quad (28)$$

$$v \leq v^*,$$

$$R_x \geq R_x^*,$$

$$\text{and} \quad \left(\frac{\sigma_{11}}{\sigma_{11c}} \right)^2 + \frac{\sigma_{12}^2}{\sigma_{12c}^2} + \left(\frac{\sigma_{22}}{\sigma_{22c}} \right)^2 + \frac{\sigma_{23}^2}{\sigma_{23c}^2} \leq 1$$

Along $y = c/2a$

$$\begin{aligned} n=1 \quad & \tau_{xy} = \tau_{yz} \quad (\omega_y = \tau_{yz}^{1-2}/2) \quad \tau_{xy} = \tau_{yz} = 0 \\ n=2 \quad & \tau_{xy} = 0 \end{aligned} \quad (87)$$

The following displacement functions satisfy the boundary conditions eqs. (87) exactly,

$$\begin{aligned} u &= \sum \sum a_{mn} \sin \frac{m\pi x}{a} \sin \frac{n\pi y}{b} \\ v &= \sum \sum b_{mn} \cos \frac{m\pi x}{a} \sin \frac{n\pi y}{b} \\ w &= \sum \sum c_{mn} \sin \frac{m\pi x}{a} \sin \frac{n\pi y}{b} \end{aligned} \quad (88)$$

Substituting Eq. (88) in Eqs. (86a-d) we get Eq. (15) as an expression for the buckling load, where T_{mn} are defined by Eq. (11), except T_{11} and T_{22} which are as follows:

$$\begin{aligned} T_{11} &= \left[2a_{11} n^2 \pi^2 + a_{22} n^2 \pi^2 (a_2/a)^2 \right] a \pi (a_2/a) \\ T_{22} &= - \left[b_{11} n^2 + 2a_{22} n^2 + (a_2/a)^2 \right] a \pi^2 \end{aligned} \quad (89)$$

Deflection under transverse loading is given by Eq. (13), in which, T_{11} and T_{22} are defined in Eq. (89).

4.3.2 CONSTRAINTS AND PENALTY FUNCTIONS

The following constraints are employed in the integer penalty formulation approach for the optimization

$$q_1 = 1 - \tau_1/\tau_2 \quad \text{for } 1/2 \quad (66)$$

$$q_{1+2}/2 = \tau_1/\tau_2 = 1 \quad \text{for } 1/2 \quad (67)$$

$$q_{1+2} = 1 - \tau_1/\tau_2 \quad \text{for } 1/2 \quad (68)$$

$$q_{1+2} = 1 - \tau_1/\tau_2 \quad \text{for } 1/2 \quad (69)$$

$$\tau_{2n+1} = 1 - \tau_1/\tau_2 \quad (70)$$

$$\tau_{2n+2} = \tau_1/\tau_2 = 1 \quad (71)$$

and

$$\tau_{1+2n+2} = 1 - \left(\frac{\partial L}{\partial \tau_{1+2n+2}} \right) \tau_1 + \frac{\partial L}{\partial \tau_{1+2n+2}} \left(\frac{\partial L}{\partial \tau_1} \right) \tau_2 \quad (72)$$

The derivatives of the constraints in Eqs. (66) to (69) can easily be obtained and the derivatives of Eqs. (70) to (72) are given by Eqs. (30), (71), (68), (32), (72) and Eqs. (60), (61) and (74) respectively.

For problem P_1 , the constraints (66), (68) are not considered because the fiber orientations are pre-assigned and the thickness of plies are only design variables.

4.4 Minimum Weight Laminate Design

4.4.1 Design

Minimum weight considerations of an orthotropic laminated composite plate is carried out, for varying number of plies and aspect ratio, for GFRP/epoxy composite whose material properties are as given in section 3.4.1.

Minimum weight design with given properties and the following set of constraints :

Longitudinal tensile strength = 100.83 kg/sq.cm.
 Transverse tensile strength = 8.43 kg/sq.cm.
 Longitudinal compressive strength = 28.13 kg/sq.cm.
 Transverse compressive strength = 28.13 kg/sq.cm.
 Shear strength = 12.65 kg/sq.cm.
 Applied uniform transverse load = 0.005 kg/sq.cm.
 Upper limit on maximum deflection = 3.05 mm
 Minimum buckling load in x-direction = 0.00 kg/cm.
 Minimum thickness of each ply = 0.125 mm.
 Maximum thickness of each ply = 1.5 mm.

Table 4.1 shows that for a four ply unsymmetric laminate a thickness ratio of 0.438 is suitable as optimum design. The fiber orientation of approximately 10° results in minimum weight design for an aspect ratio of 0.5 and $b = 0.1$.

The variations in ply thickness with increasing number of plies is shown in Figs. 4.2 and 4.3 for an aspect ratio of 0.5 and 0.5 and an aspect ratio of 0.5 and 0.5, respectively.

Table 4.4 gives fiber thickness distribution for different pre-designed fiber configurations. The maximum fraction of the total thickness is shown by the ratio of plies with optimum fiber concentration. All other plies contain smaller assigned thickness.

Fig. 4.1 presents the variation in ply thickness ratio with increasing number of plies. The thickness ratio of outer plies approaches an asymptotic value. It approaches unity if the constraint on relative thickness is active. For every ply weight is possible, if the weight of plies is very high. The inner ply thickness ratios are very close to unity and remain almost constant.

The above results are for a pre-designed fiber configuration. Table 4.5 shows the variations of the optimum fiber concentration and corresponding thickness with aspect ratio and biaxial loading ratio. The optimum weight increases with increasing aspect ratio and biaxial loading ratio. The thickness ratio decreases with increasing biaxial loading ratio. However, the

change in the thickness ratio with increasing loading stress diminishes as the aspect ratio approaches unity. The thickness ratio decreases with increasing aspect loading ratio for ratios greater than unity. It seems that the fiber orientation angle ratio increases with increasing aspect ratio. Approximate curves for the aspect ratio and the thickness loading ratio are presented in this table.

Table 4.4 presents the variations in the ply thickness and the corresponding fiber orientations with increasing number of plies. The fiber orientation of plies near the mid-ply, approaches zero with the corresponding thickness approaching the constant assigned value.

4.4.3. MINIMUM WEIGHT

The optimum thickness ratio at the minimum weight is 2.614 for the four ply anisymmetric laminated plate. This thickness ratio is identical with the one obtained by Sharma, et. al. (16) to remove coupling effects. The thickness ratios for simply anisymmetric case are also in accordance with results of reference (16), whose version is reproduced here

$$k_2 = |k_1 - 1| \pm \sqrt{12k_1^2 - 3} \quad (92)$$

where

$$\lambda_2 = \gamma_2 / \gamma_1$$

and

$$\lambda_3 = \gamma_3 / \gamma_1$$

where γ_1 is the first component of the vector γ and γ_2, γ_3 are the second and third components, respectively. The optimal weight obtained in the above calculations in the case as is specified in the previous paragraph, and the corresponding stiffness coefficients are reduced at once by means of a given factor, which is determined by the values given in chapter 2 to get the optimum with respect to fiber orientation apply (see, for example,

the increase in the number of plies with a significant change in thickness distribution for the optimum weight considered earlier with increasing number of plies. As the number of plies increases, the laminate is identical to the one with orthotropic laminae.

In the case thickness and the corresponding fiber orientations are taken as the design variables, then the laminate with higher number of plies tends to approach the configuration of four-ply antisymmetric laminate.

The variations of the optimum weight with the

average ratio and the standard deviation is shown in Table 4.3. The explanation given in Section 4.1.

4.3. CONCLUSIONS

The following conclusions are drawn from the results obtained :

- (1) A particular thickness distribution results in the apparent weight factor for the investigated fibre orientation for any fibre size.
- (2) When the thickness and the fibre orientation are taken as the degree variables, it appears that in addition to the workable range approximated as optimum value, the range of other orientations also appeared as optimum.
- (3) The general conclusions given in Tables 1 and 2 are also applicable here as discussed in Section 4.4.2.

ANALYTICAL DATA

Total number of pulses = 1

Frequency ratio = 0.1

$\log \sqrt{P_1/P_2}$ = 0.1

Observation	Sensitivity Factor		Optimum Sensitivity ($\mu\text{V}/\mu\text{A}$)	τ_1/τ_2
	τ_1	τ_2		
$\pm 30^\circ$	0.1003	0.1000	0.1000	0.916
$\pm 10^\circ$	0.1010	1.0000	0.0112	0.916
$\pm 10^\circ$	0.1000	0.1000	0.0000	0.916

$\log_{10} \gamma_{\pm}$ — \log_{10}
aqueous ionic interaction = 2.46

Osmol molal solution	Cellular interactions										Osmotic pressure M ₂ = 2
	γ_1	γ_2	γ_3	γ_4	γ_5	γ_6	γ_7	γ_8	γ_9	γ_{10}	
1	0.94871	1.0000									4.12940
2	0.94871	0.99999	0.99999								4.12938
3	0.94871	0.99998	0.99998	0.99999							4.12932
4	0.94871	0.99997	0.99997	0.99998	0.99999						4.12924
5	0.94871	0.99996	0.99996	0.99997	0.99998	0.99999					4.12916
6	0.94871	0.99995	0.99995	0.99997	0.99998	0.99999	0.99999				4.12908
7	0.94871	0.99994	0.99994	0.99996	0.99997	0.99998	0.99999	0.99999			4.12900
8	0.94871	0.99993	0.99993	0.99995	0.99996	0.99997	0.99998	0.99999	0.99999		4.12892
9	0.94871	0.99992	0.99992	0.99994	0.99995	0.99996	0.99997	0.99998	0.99999	0.99999	4.12884
10	0.94871	0.99991	0.99991	0.99993	0.99994	0.99995	0.99996	0.99997	0.99998	0.99999	4.12876
20	0.94871	0.99990	0.99990	0.99992	0.99993	0.99994	0.99995	0.99996	0.99997	0.99998	4.12868

$\log_{10} \gamma_{\pm} = \log_{10} \gamma_{\pm}^{\text{cellular}}$

Reynolds ratio

$= 0.5$

$\kappa = \eta / \eta_{\infty}$

$= 0.5$

Maximum shear rate $\dot{\gamma}_{max} = 4.10$

Shear rate [s ⁻¹]	Optimal structure										Optimal viscosity [Pa·s]
	γ_1	γ_2	γ_3	γ_4	γ_5	γ_6	γ_7	γ_8	γ_9	γ_{10}	
1	0.3020	0.6466									2.6032
5	0.3020	0.6104	0.4831								2.6030
10	0.2768	0.6400	0.5530	0.5078							2.6032
15	0.2648	0.6700	0.5985	0.5861	0.5008	0.3287					2.6033
20	0.2648	0.6713	0.6500	0.6830	0.5503	0.5099	0.3580	0.2533			2.6030
30	0.2673	0.6834	0.6800	0.7378	0.5707	0.5508	0.4000	0.5873	0.1384	0.1383	2.6030

Support angle θ_0	μ $\frac{h_0}{h_1}$	Spectrum values				Optimum bracket width mm	Actual bracket width	$\frac{h_1}{h_2}$	$\frac{\alpha_1}{\alpha_2}$
		γ_1	γ_2	α_1	α_2				
0.0	0.0	0.000	0.000	0.00	-0.00	0.57	unloading	1.0	-0.0
	0.5	-0.001	-0.001	0.00	-0.00	0.66	unloading	0.94	-0.05
	1.0	-0.004	-0.004	0.00	-0.00	0.80	unloading	0.89	-0.09
0.5	0.0	0.000	0.000	0.00	-0.00	0.39	unloading	0.86	-0.04
	0.5	0.001	0.001	0.00	-0.00	0.44	unloading	0.88	-0.06
	1.0	0.007	0.007	0.00	-0.00	0.61	unloading	0.89	-0.09
1.0	0.0	0.000	0.000	0.00	-0.00	0.01	unloading	0.89	-0.09
	0.5	0.007	0.007	0.00	-0.00	0.01	unloading	0.89	-0.09
	1.0	0.006	0.006	0.00	-0.00	0.01	unloading	0.89	-0.09
2.0	0.0	0.000	0.000	0.00	-0.00	0.00	unloading	0.89	-0.09

$$\text{segment ratio} = 1.0$$

$$x = \frac{V_1}{V_1 + V_2} \quad n = 2.0$$

Trial Number or Point	Optimum values						Type Specimen No.
	V_1/V_2	V_1/V_3	V_1/V_4	V_1/V_5	V_1/V_6	V_1/V_7	
4	0.5807	0.4322					4.01
	08.10	-45.44					
5	0.5057	1.2845	0.1230				4.04
	44.93	-14.96	-0.47				
6	0.5044	0.0348	0.5301	0.1401			4.03
	44.33	-35.04	-41.90	1.37			
19	0.4333	0.0207	0.1629	0.0807	0.0009		4.06
	42.72	-34.79	-33.59	-2.10	-0.94		
12	0.3874	-0.7353	0.1506	0.1920	0.0485	0.1580	4.09
	-45.85	49.09	-0.86	5.02	3.09	9.45	

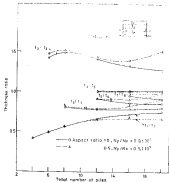


FIG. 4.7. THICKNESS RATIO VS. TOTAL NUMBER OF PILES

CHAPTER 2

INTRODUCTION

The key to the effective design of composite structures is the proper use of the optimization techniques for more efficient utilization of the material. An unfortunate circumstance which restricts the maximum use of all the design flexibilities provided by composites is the intrinsic complexities involved at micro-mechanical and macro-mechanical levels of the analysis of such materials. However, lot of theoretical advancements have been made and the usage of optimization techniques is gaining momentum.

In order to comprehend and appreciate the vital role which the application of optimization techniques can play, it is worthwhile to point out here, that a reduction by one-tenth of a millimeter of thickness, for a plate of size 10' x 50', results in material cost-savings of approximately 1-10 % (for epoxy composite cost projection, as present). This alone may indicate the operational cost-savings, which will be tremendous in the case of aerospace applications.

In this thesis, the optimization studies have been carried out, incorporating a set of design variables to achieve more flexibility in the design, to get a

maximum weight design of a laminated composite plate. Particular cases of laminates with specially orthotropic laminae and bi-layered and angle-ply laminates were considered. Maximum flexibility in choosing the design variables was realized while restricting the analysis to analytical frameworks to avoid numerical techniques, which, besides being approximate as shown are also time consuming. Simply supported boundary conditions which are amenable to closed form solutions have been used throughout the study.

In the following chapters, the conclusions drawn at the end of each chapter is summarized.

The constrained optimization problem is transformed into a series of unconstrained optimization problems, using interior penalty function approach. It should be noted that the filter constraints (design variables) enter the transformed function through the constraints. Objective function does not contain the filter orientations as variables. For higher values of the penalty parameter, some of the constraints become active. (transformed objective function has the minimum over each the constraint surfaces) or in other words, behaviour of each side constraint contribute almost equally to the objective function. This results in the filter orientations achieving an optimum value, with every constraint contributing almost equally

to it. During numerical optimization, when the penalty parameter is reduced to a lower value, the active constraint contributes dominantly to the objective function. Due to this, the fitted orientation of the inner plate, whose positions are, in comparison with other variations, may not reach the optimum value. This does not affect the optimum weight appreciably.

The total computational time taken by the algorithm is dependent on the design point, the exact optimum value and other factors. In view of this, any comparison of total computational time is not attempted. Mesh stress and deflection analysis takes about 0.13 second and, if analytical derivatives are calculated, an additional time of about 0.07 second is taken. For calculating the numerical derivatives, the algorithm takes about 0.88 second. Hence, analytical derivatives calculation results in less CPU (Central Processing Unit) time.

The following general conclusions can be drawn from the study conducted :

- (1) Maximum buckling load is obtained when the total thickness of the plate assumes the optimum fiber orientation for a given aspect ratio and biaxial loading ratio.

- (2) The designer of the composite plate can work with related strengthening techniques, to sit as plates near the mid-plane are considered.
- (3) The weight per unit area of the plate decreases with increasing aspect ratio. However, its area to support an assigned value with aspect ratio.
- (4) Curious stress history results at option A with the low deflection requirement on the laminated design. These constraints can be deleted to improve the efficiency of the structure.
- (5) The optimum for an antisymmetric angle-ply laminate is obtained when the ply thicknesses achieve particular ratios.

EXTENSION OF THE PRESENT WORK

The logical extension of the present work can be stated as follows :

- (1) A general unsymmetric laminated ply can be considered with various boundary conditions.
- (2) Volume fraction of the fiber and the matrix of each ply can be incorporated as a design variable to get an optimum weight structure.
- (3) Optimization of hybrid laminates.

REFERENCES

- (1) Kise, L., "Optimal design of structures of composite materials", *International J of Solids and Structures*, Vol. 8, No. 7, 1972, pp. 888 - 890.
- (2) Krygashin, N.B., "On the dynamic stability analysis of ^{FB}isotropic viscoelastic bodies", *J of Applied Mathematics and Mechanics*, Vol. 35, No. 4, 1973, pp. 714 - 718.
- (3) Laro, R.G., and Lashin, N.B., "On the theory of optimal constant thickness fiber reinforced plates", *International J of Mechanical Sciences*, Vol. 15, 1973, pp. 331 - 338.
- (4) Kise, L.B., and Vashkov, V.G., Gerasim, G., and Tsakir, Y., "Optimization of fiber reinforced composite structures", *International J of Solids and Structures*, Vol. 9, 1973, pp. 1821 - 1828.
- (5) Lai, Y.S., and Kachutsky, A.A., "Optimal design of layered structures under dynamic loading", *Composites and Structures*, Vol. 3, 1975, pp. 189 - 193.
- (6) Schmit, L.J., L.J., and Pappas, P., "Optimum structural design for strength and stiffness", *Structural J for Mechanical Engineering*, Vol. 7, No. 4, 1972, pp. 519 - 524.

- (17) Takashashi, G., Murty, R. and Sano, S., "A program for optimum design of flexible and composite structures subject to strength and deflection constraints". Proc. Symposium, structural dynamics and material conference, San Diego, California, March 29-31, 1977.
- (18) Khan, M.S., "Computer programs (DYCOM2) for optimization of composite structures for minimum weight design". U.S. Airforce Dynamic Laboratory, Tech. report DFFD-68-76-148, 1977, pp. 14.
- (19) McKeown, J.J., "Optimal composite structures by deflection variable programming". Computer Methods in Applied Mechanics and Engineering, Vol. 12, 1977, pp. 175-178.
- (20) McKeown, J.J., "A new approach to the optimization of laminar composite beams". Proc. International Journal of Aeronautical Science conference 1978, Lisbon, Portugal, Sept. 10-14, 1978, Vol. 1.
- (21) McKeown, J.J., "A quasi-linear programming algorithm for optimizing stress - reinforced structures of fixed stiffness". Computer Methods in Applied Mechanics and Engineering, Vol. 8, 1978, pp. 133-154.

- [15] Choe, G.G., Koh, S.H. and Son, S.L., "Buckling and yield strengths of laminated composites", *Adv. Design*, Vol. 13, No. 2, 1978, pp. 1131 - 1138.
- [16] Schmit, G.L., S.A. and Furst, S., "Optimum design of laminated fiber composite plates", *International J. for Numerical Methods in Engineering*, Vol. 11, no. 4, 1977, pp. 833-847.
- [17] Koyachi, T., "Optimization and elastic buckling strength of fiber reinforced composite structures: columns, plates and cylinders", *Proceedings of symposium*, Kyoto, Society of Material Science Japan, 1974, pp. 399-409.
- [18] Hsiao, T., "Optimum design of laminated plates under axial compression", *Adv. Design*, Vol. 17, 1979, pp. 1017-1018.
- [19] Shama, S., Tzeng, S.G.H. and Hsieh, S.H., "Some comments on analysis of angle ply laminates", *J. structural mechanics*, Vol. 7, 1979, pp. 473-483.
- [20] Brinson, L.C. and Kress, R.H., Ed. "Composite Materials" Vol. 3, Academic Press, 1974.
- [21] Tzeng, S.G.H. and Cheng, S.H., "Programming methods in structural design" *Affiliated East-West Press Private Limited, Delhi*, 1980.

- (18) Dodge, R.H., "Regulation of corporate management
American economic company, 1973.
- (19) Dodge, R.H., "The regulation of financial corporate
companies", in American economic company,
New York, 1973.

APPENDIX 1

The gradients of the stiffness matrices are obtained in the following manner:

$$\frac{\partial \hat{B}_{1,j}}{\partial \hat{u}_1} = \frac{\partial}{\partial \hat{u}_1} \left[\frac{\partial \hat{B}_{1,j}}{\partial \hat{u}_n} (\hat{u}_n - \hat{u}_{n-1}) \right] = \hat{B}_{1,j} \left(\frac{\partial \hat{u}_n}{\partial \hat{u}_1} - \frac{\partial \hat{u}_{n-1}}{\partial \hat{u}_1} \right)$$

$$\begin{aligned} \frac{\partial \hat{B}_{1,j}}{\partial \hat{u}_1} &= \frac{\partial}{\partial \hat{u}_1} \left[\frac{1}{2} + \frac{\partial \hat{B}_{1,j}}{\partial \hat{u}_{n-1}} (\hat{u}_n^2 - \hat{u}_{n-1}^2) \right. \\ &\quad \left. + \hat{B}_{1,j}^{(2)} \left(\hat{u}_n^2 \frac{\partial \hat{u}_n}{\partial \hat{u}_1} - \hat{u}_{n-1}^2 \frac{\partial \hat{u}_{n-1}}{\partial \hat{u}_1} \right) \right] \end{aligned}$$

$$\begin{aligned} \frac{\partial \hat{B}_{1,j}}{\partial \hat{u}_1} &= \frac{\partial}{\partial \hat{u}_1} \left[\frac{1}{2} + \frac{\partial \hat{B}_{1,j}}{\partial \hat{u}_{n-1}} (\hat{u}_n^2 - \hat{u}_{n-1}^2) \right. \\ &\quad \left. + \hat{B}_{1,j}^{(2)} \left(\hat{u}_n^2 \frac{\partial \hat{u}_n}{\partial \hat{u}_1} - \hat{u}_{n-1}^2 \frac{\partial \hat{u}_{n-1}}{\partial \hat{u}_1} \right) \right] \end{aligned}$$

where

$$\begin{aligned} \hat{u}_1 &= \hat{u}_n && \text{for } \text{ord} = 1, 3^{\text{rd}}/2 \\ & && \text{ord} = 3 \\ \hat{u}_1 &= \hat{u}_n && \text{for } 2\text{ord}/2\text{ord} = 2^{\text{nd}} \\ & && \text{ord} = 2, 4^{\text{th}} \end{aligned}$$

and

$$\frac{\partial \hat{B}_{1,j}}{\partial \hat{u}_{n-1}} = 0 \quad \text{for } \text{ord} = 1$$

and

$$\frac{\partial \mathcal{E}_{12}^{(k)}}{\partial \mathcal{K}_n} = -\pi_2 \sin \left(2 \mathcal{K}_n \right) - 4 \pi_3 \sin \left(4 \mathcal{K}_n \right)$$

$$\frac{\partial \mathcal{E}_{12}^{(k)}}{\partial \mathcal{K}_n} = 4 \pi_3 \sin \left(4 \mathcal{K}_n \right)$$

$$\frac{\partial \mathcal{E}_{12}^{(k)}}{\partial \mathcal{K}_n} = 2 \pi_2 \sin \left(2 \mathcal{K}_n \right) + 4 \pi_3 \sin \left(4 \mathcal{K}_n \right)$$

$$\frac{\partial \mathcal{E}_{12}^{(k)}}{\partial \mathcal{K}_n} = \pi_2 \cos \left(2 \mathcal{K}_n \right) + 4 \pi_3 \cos \left(4 \mathcal{K}_n \right)$$

$$\frac{\partial \mathcal{E}_{23}^{(k)}}{\partial \mathcal{K}_n} = \pi_2 \cos \left(2 \mathcal{K}_n \right) - 4 \pi_3 \cos \left(4 \mathcal{K}_n \right)$$

$$\frac{\partial \mathcal{E}_{23}^{(k)}}{\partial \mathcal{K}_n} = 4 \pi_3 \sin \left(4 \mathcal{K}_n \right)$$

$$\text{for } k = n$$

where

$$\pi_2 = \frac{u_{12} - \mathcal{G}_{12}}{2}$$

$$\pi_3 = \frac{u_{12} + u_{23} - \mathcal{G}_{12} - \mathcal{G}_{23}}{2}$$

and

$$\frac{\partial \mathcal{E}_n}{\partial \mathcal{K}_n} = -\frac{1}{2} \quad \text{if } n \in \mathcal{N}$$

and $n \notin \mathcal{N}$

$$= \frac{1}{2} \quad \text{if } n \in \mathcal{N}$$

$$= 0 \quad \text{if } n \in \mathcal{N}$$

$$= -11 \quad$$

where

$$u_k = -\frac{1}{2} \sum_{j=1}^N c_j \quad k = 0$$

$$u = -\frac{1}{2} \sum_{j=1}^N b_j = -\frac{1}{2} \sum_{j=1}^N c_j \quad \text{for } 1 \leq N-1$$

$$u = -\frac{1}{2} \sum_{k=1}^N \sum_{j=1}^N b_j = -\frac{1}{2} \sum_{j=1}^N b_j \quad \text{for } N=2$$

$$u = -\frac{1}{2} \sum_{j=1}^N c_j \quad \text{for } N=1$$

$$u = 0 \quad \text{for } N=0$$

(See Fig. 3-1)